Friedman et al., 1980; Burton, 1986), and a serial feed-forward mode of somatosensory processing from SI to SII has been confirmed in monkeys (Friedman et al., 1986; Pons et al., 1987, 1992; Garraghty et al., 1990) and humans (Disbrow et al., 2001; Inui et al., 2004). Our data also indicated the peak latency of SI to be significantly earlier than that of the cSII (Figs. 6 and 7). Several investigators have also reported strong connections between SII and IPL (Pandya and Seltzer, 1982; Cavada and Goldman-Rakic, 1989; Burton, 1986; Andersen et al., 1990; Wu and Kaas, 2003). This anatomical data was also supported by our findings that the peak latency of PPC was significantly later than that of the cSII (Figs. 6 and 7). Thus, there might be a hierarchical structure for human pain processing from SI to IPL.

The second is parallel pain processing in SI and SII to IPL (Fig. 8B). Anatomical studies have provided evidence that the SII receives nociceptive projections from lateral thalamic nuclei (Friedman and Murray, 1986; Stevens et al., 1993). These projections originate mostly from the ventral posterior inferior nucleus (VPI), whereas nociceptive projections to SI originate predominantly from the VPL (Kenshalo et al., 1980; Gingold et al., 1991; reviewed in Schnitzler and Ploner, 2000; Treede et al., 2000). Thus, differences in spinal input and response characteristics of VPI and VPL neurons indicate anatomic and functional segregation of nociceptive pathways from the spinal cord to SI and SII (Apkarian and Hodge, 1989; Dong et al., 1989; Apkarian and Shi, 1994; Schnitzler and Ploner, 2000). However, our findings did not confirm this hypothesis, since the ECD peak latency of the thigh SI was significantly earlier than that of cSII (Figs. 6 and 7).

Third, two parallel streams of processing may flow in the cortical hierarchy, one from SI to IPL via area 5, and the other via SII (Fig. 8C), based on the cortico-cortical pathways in monkeys (Neal et al., 1986, 1987, 1990). The human Brodmann's areas 5/7 of PPC receives main inputs from areas 1 and 2 of SI (Pons and Kaas, 1986), and it has been shown that area 5 sends cortico-cortical fibers to IPL as a feed-forward connection (Friedman et al., 1986; Neal et al., 1986, 1987, 1990; Cavada and Goldman-Rakic, 1989; Padberg et al., 2005). Some neuroimaging studies using PET and fMRI showed activities in both areas 5 and 40 after noxious stimulation (Hsieh et al., 1995a, 1995b; Iadarola et al., 1998; Davis et al., 2002; Niddam et al., 2002, 2008; Mainhöfner et al., 2006; Staud et al., 2007). Consequently, two parallel pathways of pain processing might exist in the human cortico-cortical network. However, this study could not directly address the third hypothesis, because we did not detect the activation of area 5.

The present study could not detect the neural activities from ACC, while some EEG studies have shown the ACC activity by using dipole modeling (Tarkka and Treede, 1993; Bromm and Chen, 1995; Valeriani et al., 1996, 2000; Garcia-Larrea et al., 2003; Schlereth et al., 2003; Tsuji et al., 2006) and intracranial recordings (Ohara et al., 2004a,b,c; Frot et al., 2008). Some MEG studies also reported small MEG activities in ACC following strong electrical stimulation (Kitamura et al., 1995), laser stimulation (Bromm et al., 1996) and noxious stimulation caused by specialized intra-epidermal needle electrode (Inui et al., 2003a). However, in a common sense, it is difficult for MEG to detect dipoles generated in the deep areas compared with EEG, and we could not find significant clear activity there in the present study, probably due to a small signal-to-noise ratio.

In addition, we could not separate the neural activities of the insula cortex from those of SII on ECD analysis. The spatial resolution of MEG is much higher than that of EEG, which cannot separate activity in the insula cortex from SII, but it seems difficult for ECD analysis in Neuromag MEG system to separate the activity between the insula and SII. On the other hand, a study reported activities in the insula, using other machines such as BTI machine (Inui et al., 2003a). This would relate to one of disadvantages of this system that activation of areas less than 2 cm apart can be difficult to discern (reviewed in Hari et al., 2000). Indeed, many pain and tactile studies using the same MEG system could not separate these activities (Ploner et al., 1999, 2000, 2002; Kanda et al., 2000; Timmermann et al., 2001; Raij et al., 2003; Wasaka et al., 2003, 2005, 2007; Nakata et al., 2004; Forss et al., 2005; Kida et al., 2006, 2007).

### *Activation of the IPL*

In humans, a number of neuroimaging studies have shown the IPL of PPC to be activated after noxious stimulation (Derbyshire et al., 1994, 1997; Hsieh et al., 1995a,b, 1996; Iadarola et al., 1998; Svensson et al., 1998; Gelnar et al., 1999; Apkarian et al., 2000; Coghill et al., 2001; Davis et al., 2002; Gracely et al., 2002; Kurata et al., 2002; Niddam et al., 2002, 2008; Dunckley et al., 2005; Mainhöfner et al., 2006; Symonds et al., 2006; Albanese et al., 2007; Staud et al., 2007; Ogino et al., 2007). In these studies, the IPL of PPC is activated by noxious stimulation more frequently than the SPL. When PPC is activated during noxious stimulation, the percentage that the activity of the IPL was identified is 94% (17/18) and 82% (14/17) in right and left hemispheres, respectively. On the other hand, the percent of the SPL is 50% (9/18) and 53% (9/17) in right and left hemispheres, respectively.

In monkey brain, the IPL is subdivided according to Vogt and Vogt (1919) into a caudal and rostral area, 7a and 7b, respectively. Anatomical evidence indicates that some neurons in the IPL including monkey area 7b, which is located in a similar region to Brodmann's area 40 in humans, responded exclusively to noxious mechanical stimulation to accurately encode stimulus duration (Dong et al., 1989, 1994; reviewed in Treede et al., 1999), and monkey area 7b also contains more neurons, which respond to nociception, than SII (Robinson and Burton, 1980). To our knowledge, we do not know any monkey studies examining the neuron activity in the IPL to laser stimulation. However, there are some fMRI and PET studies in humans that the IPL was activated by laser (Derbyshire et al., 1997) and mechanical stimulation (Gracely et al., 2002; Mainhöfner et al., 2006). Thus, we consider that IPL may play some roles in pain processing, not depending on a kind of noxious stimulation.

However, the temporal dynamics of IPL during pain processing is not well understood. Some patient data have shown that Brodmann's area 40 in IPL is related to the discrimination and sensation of pain (Schmahmann and Leifer, 1992; Bassetti et al., 1993). IPLs are polymodal association cortices with a role in pain processing, especially in orientating attention toward a noxious stimulation and the high sensory integration of pain (Dunckley et al., 2005; Oshiro et al., 2007). In addition, several neuroimaging studies revealed right lateralized activation in IPL during noxious stimulation, regardless of the side stimulated (Coghill et al., 2001; Symonds et al., 2006). According to Coghill et al. (2001), Brodmann's area 40 in IPL is activated during noxious stimulation, but is also active during non-painful thermal stimulation and not sensitive to the intensity of the thermal

stimulus (Coghill et al., 2001). The present study was not designed to evaluate the difference in activities of IPL between the right and left hemispheres after noxious stimulation of the thigh, but the data obtained using MEG confirmed the activation of IPL within the right cerebral hemisphere.

*Activation of the thigh SI*

The foot SI is located deeper, facing the interhemispheric fissure, and not on the cortical surface. Based on the structural organization of the brain, Hari et al. suggest that the foot SI is cytoarchitectonically different from the hand SI (Hari et al., 1996). They recorded somatosensory evoked magnetic fields (SEFs) after presenting tactile stimulation to the left and right tibial nerves at the ankles. Of note, they found that the dipole orientation of the foot SI changed dynamically with counterclockwise rotation. This result has been confirmed (Fujita et al., 1995; Kakigi et al., 1995b). Taking these previous studies into consideration, we were afraid of not being able to identify the activities in SI, if we presented noxious stimulation to the foot. That is, since the dipole location and orientation of the foot SI is very complicated, it is possible that MEG could not detect the activity precisely. This is because MEG has difficulty in detecting brain dipoles radial to the skull, and dipoles generated in deep areas (Kakigi et al., 2000 and Hari et al., 2000).

The present MEG study recorded the neural activity of the thigh SI after noxious stimulation. Previous neuroimaging studies using fMRI and PET have also indicated the hemodynamic response of the foot SI relating to noxious stimulation (Andersson et al., 1997; Porro et al., 1998, 2002, 2003; Chen et al., 2002; Bingel et al., 2004; Ferretti et al., 2004; Moulton et al., 2005). As shown in Table 3, the mean Talairach coordinates among these previous studies were $X$=9.2 mm, $Y$=−37.0 mm, and $Z$=64.3 mm in the right hemisphere, and $X$=−7.7 mm, $Y$=−37.7 mm, and $Z$=60.8 mm in the left hemisphere. In the present study, the mean Talairach coordinates of SI were $X$=9.1 mm, $Y$=−34.2 mm, and $Z$=56.5 mm, respectively, showing similar regions of SI to previous neuroimaging studies. SI is involved in determining the localization and intensity of a stimulus for the sensory-discriminative component of the nociceptive system, as well as the tactile system (Treede et al., 1999; Schnitzler and Ploner, 2000). Because of the limited spatial resolution of ECD estimation, we could not refer to the precise regions of SI, that is, which area of SI was activated after noxious stimulation of the thigh. Some MEG studies suggest the generation of a nociceptive response in area 1 (Kanda et al., 2000; Ploner et al., 2000; Inui et al., 2003b), and an EEG study using a dipole source analysis also indicated area 1 or 2 (Schlereth et al., 2003). In addition, intracortical and subdural recording studies tried to conciliate EEG and MEG findings by showing that such postcentral activity was located outside of area 3b (Kanda et al., 2000; Valeriani et al., 2004; Ohara et al., 2004a). It was suggested to arise from a more posterior area such as area 1 or 2, or deeper in area 3a. Consistent with these studies, previous studies recording neuronal activity in monkeys have revealed that nociceptive neurons in SI were frequently found at the rostral and caudal borders of area 1 (Kenshalo and Isensee, 1983; Chudler et al., 1990). On the other hand, Tommerdahl et al. using intrinsic optical imaging showed evidence that area 3a of SI was activated by nociceptive input (Tommerdahl et al., 1996, 1998). Our findings suggest that the thigh SI was activated after noxious stimulation, but further studies are needed to identify the precise location.

**Table 3**
Talairach coordinates of primary somatosensory cortex (SI) evoked by noxious stimulation of the foot in previous neuroimaging studies

| | Scan | Pain stimulus | $X$ | $Y$ | $Z$ |
|---|---|---|---|---|---|
| *Right hemisphere* | | | | | |
| Porro et al. (1998) | fMRI | Ascorbic acid, saline | 7 | −40 | 60 |
| Chen et al. (2002) | fMRI | Contact heat | 16 | −35 | 68 |
| Porro et al. (2002) | fMRI | Ascorbic acid | 10 | −35 | 65 |
| Porro et al. (2003) | fMRI | Ascorbic acid, saline | 6 | −37 | 58 |
| Bingel et al. (2004) | fMRI | Laser | 9 | −36 | 66 |
| Moulton et al. (2005) | fMRI | Contact heat | 7 | −39 | 69 |
| Average | | | 9.2 | −37.0 | 64.3 |
| *Left hemisphere* | | | | | |
| Andersson et al. (1997) | PET | Capsaicin | −1 | −34 | 60 |
| Porro et al. (2002) | fMRI | Ascorbic acid | −10 | −35 | 65 |
| Porro et al. (2003) | fMRI | Ascorbic acid, saline | −6 | −37 | 58 |
| Bingel et al. (2004) | fMRI | Laser | −9 | −39 | 57 |
| Ferretti et al. (2004) | fMRI | Electrical | −4 | −42 | 59 |
| Moulton et al. (2005) | fMRI | Contact heat | −16 | −39 | 66 |
| Average | | | −7.7 | −37.7 | 60.8 |

fMRI = functional magnetic resonance imaging; PET = positron emission tomography.

*Comparison between the present study and previous MEG studies*

Some MEG studies reported a simultaneous activation of SI and SII, with peaks at a latency of about 170 ms after noxious stimulation of the hand, indicating a parallel thalamocortical distribution of nociceptive information (Ploner et al., 1999, 2000, 2002; Inui et al., 2002; Nakata et al., 2004). However, a critical issue in these studies was that the peak latency of SI was significantly and/or clearly later than that of SII, though onset latency was similar between SI and SII. Peak latency has been used to know the time course of neural activities in neurophysiological studies, such as with MEG and EEG. As for the onset latency of ECD moment waveforms, we inferred that the evaluation included a technical problem of analysis, because the onset of ECDs was defined by visual evaluation of experimenters. For example, in Fig. 6 of the present study, the evaluation of the onset was complicated in some subjects. Strictly speaking, data on the onset latency from previous MEG studies showed "almost the same latency", not "exactly the same latency". Thus, even if the onset latencies differed between SI and SII, the difference might not be reflected clearly on the ECD moment waveform. However, the peak latencies for each component were easily defined in all subjects, and the data indicated "just latency".

In addition, we considered that there are several hypotheses to interpret the delay in peak latency of SI in some previous MEG studies. One hypothesis is that the nociceptive information flowed from SII to SI. However, as indicated earlier, hierarchical somatosensory information basically flows from SI to SII in the cortex. Thus, this hypothesis can be ruled out, because of the contradictory pattern observed. A second hypothesis is that the response recorded at about 170 ms after noxious stimulation indicated the neural activity of PPC, not SI. It is possible that noxious somatosensory information flows from SII to PPC, since Forss et al. reported that a cortical pain network included SII and PPC, not SI (Forss et al., 2005). They referred to area 5/7 as the source of PPC activity. However, SII does not project at all to area 5 in monkeys (Jones and Powell, 1969; Stanton et al., 1977; Friedman et al., 1986), while some studies reported findings on projections from SII to area 5 in cats (Burton and Kopf, 1984; Avendaño et al., 1988). Thus,

direct cortical projections from SII to area 5 may not exist in the human cerebral cortex. Moreover, since a large number of studies have shown a role for SI in human pain processing (Treede et al., 2000; Treede and Lenz, 2006), further studies would be needed to clarify the second hypothesis in more detail. A third hypothesis is that the activities of the hand SI and PPC overlapped during a similar period after the stimulation, because the distance between the hand SI and PPC is anatomically very small. In Fig. 5, this notion was verified and the hand SI and PPC could not be separated after stimulation of the hand dorsum. This hypothesis does not exclude the findings of both Forss et al. (2005) and those of some MEG studies showing the activity of SI. We considered that the location of the ECD should change for each subject, depending on whether dipole strengths are larger for SI or PPC. The current study confirmed the third hypothesis by presenting noxious stimulation to the thigh.

## Summary

The present study investigated human pain processing using MEG following the application of a YAG laser to the left thigh. The pain-related activities were recorded in the contralateral thigh SI, IPL (Brodmann's area 40), and bilateral SII. The mean peak latencies of SI, cSII, iSII, and IPL were 152, 170, 181, and 183 ms, respectively. The differences of peak latencies among these activities indicated a serial mode of pain processing from SI to IPL, and the time course of each activated region.

## Acknowledgments

We are grateful to Mr. O. Nagata and Mr. Y. Takeshima for technical help during the study. This study was supported by grants from the Japan Society for the Promotion of Science for Young Scientists to H.N., and by Research on Psychiatric and Neurological Diseases and Mental Health.

## References

Akatsuka, K., Wasaka, T., Nakata, H., Kida, T., Kakigi, R., 2007a. The effect of stimulus probability on the somatosensory mismatch field. Exp. Brain Res. 181, 607–614.
Akatsuka, K., Wasaka, T., Nakata, H., Kida, T., Hoshiyama, M., Tamura, Y., Kakigi, R., 2007b. Objective examination for two-point stimulation using a somatosensory oddball paradigm: an MEG study. Clin. Neurophysiol. 118, 403–411.
Albanese, M.C., Duerden, E.G., Rainville, P., Duncan, G.H., 2007. Memory traces of pain in human cortex. J. Neurosci. 27, 4612–4620.
Andersen, R.A., Asanuma, C., Essick, G., Siegel, R.M., 1990. Corticocortical connections of anatomically and physiologically defined subdivisions within the inferior parietal lobule. J. Comp. Neurol. 296, 65–113.
Andersson, J.L., Lilja, A., Hartvig, P., Långström, B., Gordh, T., Handwerker, H., Torebjörk, E., 1997. Somatotopic organization along the central sulcus, for pain localization in humans, as revealed by positron emission tomography. Exp. Brain Res. 117, 192–199.
Apkarian, A.V., Hodge, C.J., 1989. Primate spinothalamic pathways: II. The cells of origin of the dorsolateral and ventral spinothalamic pathways. J. Comp. Neurol. 288, 474–492.
Apkarian, A.V., Shi, T., 1994. Squirrel monkey lateral thalamus. I. Somatic nociresponsive neurons and their relation to spinothalamic terminals. J. Neurosci. 14, 6779–6795.
Apkarian, A.V., Gelnar, P.A., Krauss, B.R., Szeverenyi, N.M., 2000. Cortical responses to thermal pain depend on stimulus size: a functional MRI study. J. Neurophysiol. 83, 3113–3122.
Avendaño, C., Rausell, E., Perez-Aguilar, D., Isorna, S., 1988. Organization of the association cortical afferent connections of area 5: a retrograde tracer study in the cat. J. Comp. Neurol. 278, 1–33.
Avikainen, S., Forss, N., Hari, R., 2002. Modulated activation of the human SI and SII cortices during observation of hand actions. NeuroImage 15, 640–646.
Bassetti, C., Bogousslavsky, J., Regli, F., 1993. Sensory syndromes in parietal stroke. Neurology 43, 1942–1949.
Bingel, U., Lorenz, J., Gläuche, V., Knab, R., Glascher, J., Weiller, C., Büchel, C., 2004. Somatotopic organization of human somatosensory cortices for pain: a single trial fMRI study. NeuroImage 23, 224–232.
Bonte, M., Parviainen, T., Hytönen, K., Salmelin, R., 2006. Time course of top–down and bottom–up influences on syllable processing in the auditory cortex. Cereb. Cortex 16, 115–123.
Bromm, B., Chen, A.C., 1995. Brain electrical source analysis of laser evoked potentials in response to painful trigeminal nerve stimulation. Electroencephalogr. Clin. Neurophysiol. 95, 14–26.
Bromm, B., Lorenz, J., 1998. Neurophysiological evaluation of pain. Electroencephalogr. Clin. Neurophysiol. 107, 227–253.
Bromm, B., Lorenz, J., Scharein, E., 1996. Dipole source analysis of brain activity in the assessment of pain. In: Kimura, J., Shibasaki, H. (Eds.), Recent Advances in Clinical Neurophysiology. Elsevier, Amsterdam, pp. 328–335.
Burton, H., 1986. Second somatosensory cortex and related areas. In: Jones, E.G., Peters, A. (Eds.), Cerebral Cortex, Vol 5. Plenum Press, New York, pp. 31–98.
Burton, H., Kopf, E.M., 1984. Ipsilateral cortical connections from the second and fourth somatic sensory areas in the cat. J. Comp. Neurol. 225, 527–553.
Carpenter, M.B., Sutin, J., 1983. Human anatomy, 8th ed. Williams & Wilkins, Baltimore.
Cavada, C., Goldman-Rakic, P.S., 1989. Posterior parietal cortex in rhesus monkey: I. Parcellation of areas based on distinctive limbic and sensory corticocortical connections. J. Comp. Neurol. 287, 393–421.
Chen, J.I., Ha, B., Bushnell, M.C., Pike, B., Duncan, G.H., 2002. Differentiating noxious- and innocuous-related activation of human somatosensory cortices using temporal analysis of fMRI. J. Neurophysiol. 88, 464–474.
Chudler, E.H., Anton, F., Dubner, R., Kenshalo Jr., D.R., 1990. Responses of nociceptive SI neurons in monkeys and pain sensation in humans elicited by noxious thermal stimulation: effect of interstimulus interval. J. Neurophysiol. 63, 559–569.
Coghill, R.C., Talbot, J.D., Evans, A.C., Meyer, E., Gjedde, A., Bushnell, M.C., Duncan, G.H., 1994. Distributed processing of pain and vibration by the human brain. J. Neurosci. 14, 4095–4108.
Coghill, R.C., Gilron, I., Iadarola, M.J., 2001. Hemispheric lateralization of somatosensory processing. J. Neurophysiol. 85, 2602–2612.
Culham, J.C., Kanwisher, N.G., 2001. Neuroimaging of cognitive functions in human parietal cortex. Curr. Opin. Neurobiol. 11, 157–163.
Davis, K.D., Pope, G.E., Crawley, A.P., Mikulis, D.J., 2002. Neural correlates of prickle sensation: a percept-related fMRI study. Nat. Neurosci. 5, 1121–1122.
Derbyshire, S.W., Jones, A.K., Devani, P., Friston, K.L., Feinmann, C., Harris, M., Pearce, S., Watson, J.D., Frackowiak, R.S., 1994. Cerebral responses to pain in patients with atypical facial pain measured by positron emission tomography. J. Neurol. Neurosurg. Psychiatry 57, 1166–1172.
Derbyshire, S.W., Jones, A.K., Gyulai, F., Clark, S., Townsend, D., Firestone, L.L., 1997. Pain processing during three levels of noxious stimulation produces differential patterns of central activity. Pain 73, 431–445.
Disbrow, E., Roberts, T., Poeppel, D., Krubitzer, L., 2001. Evidence for interhemispheric processing of inputs from the hands in human S2 and PV. J. Neurophysiol. 85, 2236–2244.
Dong, W.K., Salonen, L.D., Kawakami, Y., Shiwaku, T., Kaukoranta, E.M., Martin, R.F., 1989. Nociceptive responses of trigeminal neurons in SII-7b cortex of awake monkeys. Brain Res. 484, 314–324.
Dong, W.K., Chudler, E.H., Sugiyama, K., Roberts, V.J., Hayashi, T., 1994. Somatosensory, multisensory, and task-related neurons in cortical area 7b (PF) of unanesthetized monkeys. J. Neurophysiol. 72, 542–564.
Dunckley, P., Wise, R.G., Aziz, Q., Painter, D., Brooks, J., Tracey, I., Chang, L., 2005. Cortical processing of visceral and somatic stimulation: differentiating pain intensity from unpleasantness. Neuroscience 133, 533–542.
Ferretti, A., Del Grarra, C., Babiloni, C., Caulo, M., Arienzo, D., Tartaro, A., Rossini, P.M., Romani, G.L., 2004. Functional topography of the secondary somatosensory cortex for nonpainful and painful stimulation of median and tibial nerve: an fMRI study. NeuroImage 23, 1217–1225.
Forss, N., Hari, R., Salmelin, R., Ahonen, A., Hämäläinen, M., Kajola, M., Knuutila, J., Simola, J., 1994. Activation of the human posterior parietal cortex by median nerve stimulation. Exp. Brain Res. 99, 309–315.
Forss, N., Merlet, I., Vanni, S., Hämäläinen, M., Mauguière, F., Hari, R., 1996. Activation of human mesial cortex during somatosensory target detection task. Brain Res. 734, 229–235.
Forss, N., Hietanen, M., Salonen, O., Hari, R., 1999. Modified activation of somatosensory cortical network in patients with right-hemisphere stroke. Brain 122, 1889–1899.
Forss, N., Raji, T.T., Seppa, M., Hari, R., 2005. Common cortical network for first and second pain. NeuroImage 24, 132–142.
Friedman, D.P., Murray, E.A., 1986. Thalamic connectivity of the second somatosensory area and neighboring somatosensory fields of the lateral sulcus of the macaque. J. Comp. Neurol. 252, 348–373.
Friedman, D.P., Jones, E.G., Burton, H., 1980. Representation pattern in the second somatic sensory area of the monkey cerebral cortex. J. Comp. Neurol. 192, 21–41.
Friedman, D.P., Murray, E.A., O, 'Neill, J.B., Mishkin, M., 1986. Cortical connections of the somatosensory fields of the lateral sulcus of macaques: evidence for a corticolimbic pathway for touch. J. Comp. Neurol. 252, 323–347.
Frot, M., Mauguière, F., Magnin, M., Garcia-Larrea, L., 2008. Parallel processing of nociceptive A-delta inputs in SII and midcingulate cortex in humans. J. Neurosci. 28, 944–952.
Fujita, S., Nakasato, N., Matani, A., Tamura, I., Yoshimoto, T., 1995. Short latency somatosensory evoked field for tibial nerve stimulation. Biomagnetism: Fundamental Research and Clinical Applications 95–98.
Garcia-Larrea, L., Frot, M., Valeriani, M., 2003. Brain generators of laser-evoked potentials: from dipoles to functional significance. Neurophysiol. Clin. 33, 279–292.
Garraghty, P.E., Pons, T.P., Kaas, J.H., 1990. Ablations of areas 3b (SI proper) and 3a of somatosensory cortex in marmosets deactivate the second and parietal ventral somatosensory areas. Somatosens. Mot. Res. 7, 125–135.

Gelnar, P.A., Krauss, B.R., Sheehe, P.R., Szeverenyi, N.M., Apkarian, A.V., 1999. A comparative fMRI study of cortical representations for thermal painful, vibrotactile, and motor performance tasks. NeuroImage 10, 460–482.
Gingold, S.I., Greenspan, J.D., Apkarian, A.V., 1991. Anatomic evidence of nociceptive inputs to primary somatosensory cortex: relationship between spinothalamic terminals and thalamocortical cells in squirrel monkeys. J. Comp. Neurol. 308, 467–490.
Gracely, R.H., Petzke, F., Wolf, J.M., Clauw, D.J., 2002. Functional magnetic resonance imaging evidence of augmented pain processing in fibromyalgia. Arthritis Rheum. 46, 1333–1343.
Hämäläinen, M., Hari, R., Ilmoniemi, R.J., Knuutila, J., Lounasmaa, O.V., 1993. Magnetoencephalography-theory, instrumentation, and applications to noninvasive studies of the working human brain. Rev. Mod. Phys. 65, 413–497.
Hari, R., Nagamine, T., Nishitani, N., Sato, T., Tarkiainen, A., Shibasaki, H., 1996. Time-varying activation of different cytoarchitectonic areas of the human SI cortex after tibial nerve stimulation. NeuroImage 4, 111–118.
Hari, R., Levänen, S., Raij, T., 2000. Timing of human cortical functions during cognition: role of MEG. Trend. Cogn. Sci. 4, 455–462.
Hoshiyama, M., Kakigi, R., Koyama, S., Watanabe, S., Shimojo, M., 1997. Activity in posterior parietal cortex following somatosensory stimulation in man: magnetoencephalographic study using spatio-temporal source analysis. Brain Topogr. 10, 23–30.
Hsieh, J.C., Belfrage, M., Stone-Elander, S., Hansson, P., Ingvar, M., 1995a. Central representation of chronic ongoing neuropathic pain studies by positron emission tomography. Pain 63, 225–236.
Hsieh, J.C., Ståhle-Bäckdahl, M., Hägermark, O., Stone-Elander, S., Rosenquist, G., Ingvar, M., 1995b. Traumatic nociceptive pain activates the hypothalamus and the periaqueductal gray: a positron emission tomography study. Pain 64, 303–314.
Hsieh, J.C., Hannerz, J., Ingvar, M., 1996. Right-lateralised central processing for pain of nitroglycerin-induced cluster headache. Pain 67, 59–68.
Iadarola, M.J., Berman, K.F., Zeffiro, T.A., Byas-Smith, M.G., Gracely, R.H., Max, M.B., Bennett, G.J., 1998. Neural activation during acute capsaicin-evoked pain and allodynia assessed with PET. Brain 121, 931–947.
Inui, K., Tran, T.D., Qiu, Y., Wang, X., Hoshiyama, M., Kakigi, R., 2002. Pain-related magnetic fields evoked by intra-epidermal electrical stimulation in humans. Clin. Neurophysiol. 113, 298–304.
Inui, K., Tran, T.D., Qiu, Y., Wang, X., Hoshiyama, M., Kakigi, R., 2003a. A comparative magnetoencephalographic study of cortical activations evoked by noxious and innocuous somatosensory stimulations. Neuroscience 120, 235–248.
Inui, K., Wang, X., Qiu, Y., Nguyen, B.T., Ojima, S., Tamura, Y., Nakata, H., Wasaka, T., Tran, T.D., Kakigi, R., 2003b. Pain processing within the primary somatosensory cortex in humans. Eur. J. Neurosci. 18, 2859–2866.
Inui, K., Wang, X., Tamura, Y., Kaneoke, Y., Kakigi, R., 2004. Serial processing in the human somatosensory system. Cereb. Cortex 14, 851–857.
Jones, E.G., Powell, T.P., 1969. Connexions of the somatic sensory cortex of the rhesus monkey. I. Ipsilateral cortical connexions. Brain 92, 477–502.
Jones, E.G., Burton, H., Porter, R., 1975. Commissural and cortico-cortical 'Columns' in the somatic sensory cortex of primates. Science 190, 572–574.
Kakigi, R., Koyama, S., Hoshiyama, M., Kitamura, Y., Shimojo, M., Watanabe, S., 1995a. Pain-related magnetic fields following painful $CO_2$ laser stimulation in man. Neurosci. Lett. 192, 45–48.
Kakigi, R., Koyama, S., Hoshiyama, M., Kitamura, Y., Shimojo, M., Kimura, Y., Watanabe, S., 1995b. Topography of somatosensory evoked magnetic fields following posterior tibial nerve stimulation. Electroencephalogr. Clin. Neurophysiol. 95, 127–134.
Kakigi, R., Hoshiyama, M., Shimojo, M., Naka, D., Yamasaki, H., Watanabe, S., Xiang, J., Maeda, K., Lam, K., Itomi, K., Nakamura, A., 2000. The somatosensory evoked magnetic fields. Prog. Neurobiol. 61, 495–523.
Kanda, M., Nagamine, T., Ikeda, A., Ohara, S., Kunieda, T., Fujiwara, N., Yazawa, S., Sawamoto, N., Matsumoto, R., Taki, W., Shibasaki, H., 2000. Primary somatosensory cortex is actively involved in pain processing in human. Brain Res. 853, 282–289.
Kenshalo Jr., D.R., Isensee, O., 1983. Responses of primate SI cortical neurons to noxious stimuli. J. Neurophysiol. 50, 1479–1496.
Kenshalo Jr., D.R., Giesler Jr., G.J., Leonard, R.B., Willis, W.D., 1980. Responses of neurons in primate ventral posterior lateral nucleus to noxious stimuli. J. Neurophysiol. 43, 1594–1614.
Kida, T., Wasaka, T., Inui, K., Akatsuka, K., Nakata, H., Kakigi, R., 2006. Centrifugal regulation of human cortical responses to a task-relevant somatosensory signal triggering voluntary movement. NeuroImage 32, 1355–1364.
Kida, T., Inui, K., Wasaka, T., Akatsuka, K., Tanaka, E., Kakigi, R., 2007. Time-varying cortical activations related to visual-tactile cross-modal links in spatial selective attention. J. Neurophysiol. 97, 3585–3596.
Kitamura, Y., Kakigi, R., Hoshiyama, M., Koyama, S., Shimojo, M., Watanabe, S., 1995. Pain-related somatosensory evoked magnetic fields. Electroencephalogr. Clin. Neurophysiol. 95, 463–474.
Kurata, J., Thulborn, K.R., Gyulai, F.E., Firestone, L.L., 2002. Early decay of pain-related cerebral activation in functional magnetic resonance imaging: comparison with visual and motor tasks. Anesthesiology 96, 35–44.
Lin, Y.Y., Simões, C., Forss, N., Hari, R., 2000. Differential effects of muscle contraction from various body parts on neuromagnetic somatosensory responses. NeuroImage 11, 334–340.
Mainhöfner, C., Herzner, B., Handwerker, H.O., 2006. Secondary somatosensory cortex is important for the sensory-discriminative dimension of pain: a functional MRI study. Eur. J. Neurosci. 23, 1377–1383.
Möttönen, R., Järveläinen, J., Sams, M., Hari, R., 2005. Viewing speech modulates activity in the left SI mouth cortex. NeuroImage 24, 731–737.
Moulton, E.A., Keaser, M.L., Gullapalli, R.P., Greenspan, J.D., 2005. Regional intensive and temporal patterns of functional MRI activation distinguishing noxious and innocuous contact heat. J. Neurophysiol. 293, 2183–2193.
Mouraux, A., Plaghki, L., 2007. Are laser-evoked brain potentials modulated by attending to first or second pain? Pain 129, 321–331.
Nakata, H., Inui, K., Wasaka, T., Tamura, Y., Tran, T.D., Qiu, Y., Wang, X., Nguyen, T.B., Kakigi, R., 2004. Movements modulate cortical activities evoked by noxious stimulation. Pain 107, 91–98.
Nakata, H., Inui, K., Wasaka, T., Akatsuka, K., Kakigi, R., 2005. Somato-motor inhibitory processing in humans: a study with MEG and ERP. Eur. J. Neurosci. 22, 1784–1792.
Neal, J.W., Pearson, R.C., Powell, T.P., 1986. The organization of the corticocortical projection of area 5 upon area 7 in the parietal lobe of the monkey. Brain Res. 381, 164–167.
Neal, J.W., Pearson, R.C., Powell, T.P., 1987. The cortico-cortical connections of area 7b, PF, in the parietal lobe of the monkey. Brain Res. 419, 341–346.
Neal, J.W., Pearson, R.C., Powell, T.P., 1990. The ipsilateral cortico-cortical connections of area 7b, PF, in the parietal and temporal lobes of the monkey. Brain Res. 524, 119–132.
Nevalainen, P., Ramstad, R., Isotalo, E., Haapanen, M.L., Lauronen, L., 2006. Trigeminal somatosensory evoked magnetic fields to tactile stimulation. Clin. Neurophysiol. 117, 2007–2015.
Nguyen, B.T., Tran, T.D., Hoshiyama, M., Inui, K., Kakigi, R., 2004. Face representation in the human primary somatosensory cortex. Neurosci. Res. 50, 227–232.
Niddam, D.M., Yeh, T.C., Wu, Y.T., Lee, P.L., Ho, L.T., Arendt-Nielsen, L., Chen, A.C., Hsieh, J.C., 2002. Event-related functional MRI study on central representation of acute muscle pain induced by electrical stimulation. NeuroImage 17, 1437–1450.
Niddam, D.M., Chan, R.C., Lee, S.H., Yeh, T.C., Hsieh, J.C., 2008. Central representation of hyperalgesia from myofascial trigger point. NeuroImage 39, 1299–1306.
Nishitani, N., Hari, R., 2002. Viewing lip forms: cortical dynamics. Neuron 36, 1211–1220.
Nishitani, N., Uutela, K., Shibasaki, H., Hari, R., 1999. Cortical visuomotor integration during eye pursuit and eye-finger pursuit. J. Neurosci. 19, 2647–2657.
Noguchi, Y., Inui, K., Kakigi, R., 2004. Temporal dynamics of neural adaptation effect in the human visual ventral stream. J. Neurosci. 24, 6283–6290.
Noguchi, Y., Kakigi, R., 2005. Neural mechanisms of visual backward masking revealed by high temporal resolution imaging of human brain. NeuroImage 27, 178–187.
Ogino, Y., Nemoto, H., Inui, K., Saito, S., Kakigi, R., Goto, F., 2007. Inner experience of pain: imagination of pain while viewing images showing painful events forms subjective pain representation in human brain. Cereb. Cortex 17, 1139–1146.
Ohara, S., Crone, N.E., Weiss, N., Treede, R.D., Lenz, F.A., 2004a. Cutaneous painful laser stimuli evoke responses recorded directly from primary somatosensory cortex in awake humans. J. Neurophysiol. 91, 2734–2746.
Ohara, S., Crone, N.E., Weiss, N., Vogel, H., Treede, R.D., Lenz, F.A., 2004b. Attention to pain is processed at multiple cortical sites in man. Exp. Brain Res. 156, 513–517.
Ohara, S., Crone, N.E., Weiss, N., Treede, R.D., Lenz, F.A., 2004c. Amplitudes of laser evoked potential recorded from primary somatosensory, parasylvian and medial frontal cortex are graded with stimulus intensity. Pain 110, 318–328.
Ohara, S., Crone, N.E., Weiss, N., Lenz, F.A., 2006. Analysis of synchrony demonstrates 'pain networks' defined by rapidly switching, task-specific, functional connectivity between pain-related cortical structures. Pain 123, 244–253.
Opsommer, E., Weiss, T., Miltner, W.H., Plaghki, L., 2001. Scalp topography of ultralate (C-fibres) evoked potentials following thulium YAG laser stimuli to tiny skin surface areas in humans. Clin. Neurophysiol. 112, 1868–1874.
Oshiro, Y., Quevedo, A.S., McHaffie, J.G., Kraft, R.A., Coghill, R.C., 2007. Brain mechanisms supporting spatial discrimination of pain. J. Neurosci. 27, 3388–3394.
Padberg, J., Disbrow, E., Krubitzer, L., 2005. The organization and connections of anterior and posterior parietal cortex in titi monkeys: do New World monkeys have an area 2? CerebCortex 15, 1938–1963.
Pandya, D.N., Seltzer, B., 1982. Intrinsic connections and architectonics of posterior parietal cortex in the rhesus monkey. J. Comp. Neurol. 204, 196–210.
Penfield, W., Boldrey, E., 1937. Somatic motor and sensory representation in the cerebral cortex of man as studied by electrical stimulation. Brain 60, 389–443.
Ploner, M., Schmitz, F., Freund, H.J., Schnitzler, A., 1999. Parallel activation of primary and secondary somatosensory cortices in human pain processing. J. Neurophysiol. 81, 3100–3104.
Ploner, M., Schmitz, F., Freund, H.J., Schnitzler, A., 2000. Differential organization of touch and pain in human primary somatosensory cortex. J. Neurophysiol. 83, 1770–1776.
Ploner, M., Holthusen, H., Noetges, P., Schnitzler, A., 2002. Cortical representation of venous nociception in humans. J. Neurophysiol. 88, 300–305.
Pons, T.P., Kaas, J.H., 1986. Corticocortical connections of area 2 of somatosensory cortex in macaque monkeys: a correlative anatomical and electrophysiological study. J. Comp. Neurol. 248, 313–335.
Pons, T.P., Garraghty, P.E., Friedman, D.P., Mishkin, M., 1987. Physiological evidence for serial processing in somatosensory cortex. Science 237, 417–420.
Pons, T.P., Garraghty, P.E., Mishkin, M., 1992. Serial and parallel processing of tactual information in somatosensory cortex of rhesus monkeys. J. Neurophysiol. 68, 518–527.
Porro, C.A., Cettolo, V., Franoescato, M.P., Baraldi, P., 1998. Temporal and intensity coing of painin human cortex. J. Neurophysiol. 80, 3312–3320.
Porro, C.A., Baraldi, P., Pagnoni, G., Serafini, M., Facchin, P., Maieron, M., Nichelli, P., 2002. Does anticipation of pain affect cortical nociceptive systems? J. Neurosci. 22, 3206–3214.
Porro, C.A., Cettolo, V., Francescato, M.P., Baraldi, P., 2003. Functional activity mapping of the mesial hemispheric wall during anticipation of pain. NeuroImage 19, 1738–1747.
Qiu, Y., Noguchi, Y., Honda, M., Nakata, H., Tamra, Y., Tanaka, S., Sadato, N., Wang, X., Inui, K., Kakigi, R., 2006. Brain processing of the signals ascending through unmyelinated C fibers in humans: an event-related functional magnetic resonance imaging study. Cereb. Cortex 16, 1289–1295.

Raij, T.T., Vartiainen, N.V., Jousmaki, V., Hari, R., 2003. Effects of interstimulus interval on cortical responses to painful laser stimulation. J. Clin. Neurophysiol. 20, 73–79.
Robinson, C.J., Burton, H., 1980. Somatic submodality distribution within the second somatosensory (SII), 7b, retroinsular, postauditory, and granular insular cortical areas of M. fascicularis. J. Comp. Neurol. 192, 93–108.
Sakamoto, K., Nakata, H., Kakigi, R., in press. Somatosensory evoked magnetic fields following stimulation of the tongue in humans. Clin. Neurophysiol. doi:10.1016/j.clinph.2008.03.029.
Schlereth, T., Baumgärtner, U., Magerl, W., Stoeter, P., Treede, R.D., 2003. Left-hemisphere dominance in early nociceptive processing in the human parasylvian cortex. NeuroImage 20, 441–454.
Schmahmann, J.D., Leifer, D., 1992. Parietal pseudothalamic pain syndrome. Clinical features and anatomic correlates. Arch Neurol. 49, 1032–1037.
Schnitzler, A., Ploner, M., 2000. Neurophysiology and functional neuroanatomy of pain perception. J. Clin. Neurophysiol. 17, 592–603.
Stanton, G.B., Cruce, W.L.R., Goldberg, M.E., Robinson, D.L., 1977. Some ipsilateral projections to area PF and PG of the inferior parietal lobule in monkeys. Neurosci. Lett. 6, 243–250.
Staud, R., Craggs, J.G., Robinson, M.E., Perlstein, W.M., Price, D.D., 2007. Brain activity related to temporal summation of C-fiber evoked pain. Pain 129, 130–142.
Stevens, R.T., London, S.M., Apkarian, A.V., 1993. Spinothalamocortical projections to the secondary somatosensory cortex (SII) in squirrel monkey. Brain Res. 631, 241–246.
Svensson, P., Minoshima, S., Beydoun, A., Morrow, T.J., Casey, K.L., 1997. Cerebral processing of acute skin and muscle pain in humans. J. Neurophysiol. 78, 450–460.
Svensson, P., Johannsen, P., Jensen, T.S., Arendt-Nielsen, L., Nielsen, J., Stødkide-Jørgensen, H., Gee, A.D., Baatsgaard Hansen, S., Gjedde, A., 1998. Cerebral blood-flow changes evoked by two levels of painful heat stimulation: a positron emission tomography study in humans. Eur. J. Pain 2, 95–107.
Symonds, L.L., Gordon, N.S., Bixby, J.C., Mande, M.M., 2006. Right-lateralized pain processing in the human cortex: an FMRI study. J. Neurophysiol. 95, 3823–3830.
Talairach, J., Tournoux, P., 1988. Co-Planar Stereotaxic Atlas of the Human Brain. Thieme, New York.
Tarkiainen, A., Helenius, P., Salmelin, R., 2003. Category-specific occipitotemporal activation during face perception in dyslexic individuals: an MEG study. NeuroImage 19, 1194–1204.
Tarkka, I.M., Treede, R.D., 1993. Equivalent electrical source analysis of pain-related somatosensory evoked potentials elicited by a $CO_2$ laser. J. Clin. Neurophysiol. 10, 513–519.
Timmermann, L., Ploner, M., Haucke, K., Schmitz, F., Baltissen, R., Schnitzler, A., 2001. Differential coding of pain intensity in the human primary and secondary somatosensory cortex. J. Neurophysiol. 86, 1499–1503.
Tommerdahl, M., Delemos, K.A., Vierck Jr., C.J., Favorov, O.V., Whitsel, B.L., 1996. Anterior parietal cortical response to tactile and skin-heating stimuli applied to the same skin site. J. Neurophysiol. 75, 2662–2670.
Tommerdahl, M., Delemos, K.A., Favorov, O.V., Metz, C.B., Vierck Jr., C.J., Whitsel, B.L., 1998. Response of anterior parietal cortex to different modes of same-site skin stimulation. J. Neurophysiol. 80, 3272–3283.
Treede, R.D., Kenshalo, D.R., Gracely, R.H., Jones, A.K., 1999. The cortical representation of pain. Pain 79, 105–111.
Treede, R.D., Apkarian, A.V., Bromm, B., Greenspan, J.D., Lenz, F.A., 2000. Cortical representation of pain: functional characterization of nociceptive areas near the lateral sulcus. Pain 87, 113–119.
Treede, R.D., Lenz, F.A., 2006. Passing lanes and slow lanes into the nociceptive network of the human brain. Pain 123, 223–225.
Tsuji, T., Inui, K., Kojima, S., Kakigi, R., 2006. Multiple pathways for noxious information in the human spinal cord. Pain 123, 322–331.
Valeriani, M., Rambaud, L., Mauguière, F., 1996. Scalp topography and dipolar source modelling of potentials evoked by CO2 laser stimulation of the hand. Electroencephalogr. Clin. Neurophysiol. 100, 343–353.
Valeriani, M., Restuccia, D., Barba, C., Le Pera, D., Tonali, P., Mauguière, F., 2000. Sources of cortical responses to painful $CO_2$ laser skin stimulation of the hand and foot in the human brain. Clin. Neurophysiol. 111, 1103–1112.
Valeriani, M., Barba, C., Le Pera, D., Restuccia, D., Colicchio, G., Tonali, P., Gagliardo, O., Treede, R.D., 2004. Different neuronal contribution to N20 somatosensory evoked potential and to CO2 laser evoked potentials: an intracerebral recording study. Clin. Neurophysiol. 115, 211–216.
Vogt, O., Vogt, C., 1919. Allgemeinere Ergebnisse unserer Hirnforschung. J. Psychol. Neurol. 25, 279–461.
Wasaka, T., Hoshiyama, M., Nakata, H., Nishihira, Y., Kakigi, R., 2003. Gating of somatosensory evoked magnetic fields during the preparatory period of self-initiated finger movement. NeuroImage 20, 1830–1838.
Wasaka, T., Nakata, H., Akatsuka, K., Kida, T., Inui, K., Kakigi, R., 2005. Differential modulation in human primary and secondary somatosensory cortices during the preparatory period of self-initiated finger movement. Eur. J. Neurosci. 22, 1239–1247.
Wasaka, T., Kida, T., Nakata, H., Akatsuka, K., Kakigi, R., 2007. Characteristics of sensorimotor interaction in the primary and secondary somatosensory cortices in humans: a magnetoencephalography study. Neuroscience 149, 446–456.
Watanabe, S., Kakigi, R., Koyama, S., Hoshiyama, M., Kaneoke, Y., 1998. Pain processing traced by magnetoencephalography in the human brain. Brain Topogr. 10, 255–264.
Wu, C.W., Kaas, J.H., 2003. Somatosensory cortex of prosimian Galagos: physiological recording, cytoarchitecture, and corticocortical connections of anterior parietal cortex and cortex of the lateral sulcus. J. Comp. Neurol. 457, 263–292.
Young, J.P., Herath, P., Eickhoff, S., Choi, J., Grefkes, C., Zilles, K., Roland, R.E., 2004. Somatotopy and attentional modulation of the human parietal and opercular regions. J. Neurosci. 24, 5391–5399.

Pain 137 (2008) 488–494

PAIN

www.elsevier.com/locate/pain

# Pain-related evoked potentials are modulated across the cardiac cycle

Louisa Edwards [a,*], Koji Inui [b], Christopher Ring [a], Xiaohong Wang [b], Ryusuke Kakigi [b,c]

[a] International Centre for Health and Exercise Research, University of Birmingham, Birmingham B15 2TT, UK
[b] Department of Integrative Physiology, National Institute for Physiological Sciences, Okazaki 444-8585, Japan
[c] RISTEX, Japan Science and Technology Agency, Japan

Received 27 April 2007; received in revised form 1 August 2007; accepted 8 October 2007

**Abstract**

Evidence suggests that the arterial baroreceptors modulate pain. To examine whether cortical processing of nociception is modulated by natural variations in arterial baroreceptor stimulation during the cardiac cycle, peak-to-peak amplitudes of the N2–P2 pain-related potential and pain ratings were recorded in response to noxious laser stimulation at different times during the cardiac cycle in 10 healthy males. Significant variations in the N2–P2 amplitudes occurred across the cardiac cycle, with smaller amplitudes midcycle, indicating that cortical processing of nociception was attenuated during systole compared to diastole. Pain ratings did not vary across the cardiac cycle. These data support the hypothesis that arterial baroreceptors modulate the processing of nociception during each cardiac cycle.


*Keywords:* Arterial baroreceptors; Cardiac cycle; Pain ratings; Pain-related evoked potentials

## 1. Introduction

The arterial baroreceptors are stretch receptors located in the aortic arch and carotid sinus that are naturally stimulated during systole by distension of the arterial wall by the pressure pulse wave [24]. Baroreceptor activation has been shown to inhibit sensory [18] and motor [23] processes. Mounting evidence indicates that pain and nociception also vary with baroreceptor activity. Using the nociceptive flexion reflex, a polysynaptic spinal reflex that facilitates withdrawal from noxious stimuli to avoid tissue injury [39], a series of studies found that nociception was attenuated during systole, when the baroreceptors are most active, compared to diastole [2,13–15,26]. In contrast, concurrent pain ratings did not vary across the cardiac cycle [13–15]. However, pain was attenuated when the carotid baroreceptors were artificially stimulated, beyond the normal physiological range, by neck suction (for review, see [33]).

Studies have also examined the effects of neck suction on pain-related evoked brain potentials comprising a negativity (N2) followed by a positivity (P2). These potentials correlate with both pain reports and stimulus intensity [9] and are attenuated by centrally-acting analgesics [41], and therefore, have been interpreted as reflecting the cognitive processing of a noxious stimulus [20]. Both N2 and P2 amplitudes [28] and the peak-to-peak N2–P2 amplitude [3] elicited by noxious intracutaneous electrical stimulation of the finger were found to be attenuated by neck suction. However, another study has reported that the N2–P2 amplitude was augmented by neck suction [5]. Accordingly, these studies indicate that stimulation of the arterial baroreceptors can modulate processing of noxious stimuli.

To date, no studies have investigated whether natural variations in baroreceptor stimulation across the cardiac

* Corresponding author. Tel.: +44 121 415 8785; fax: +44 121 414 4121.
*E-mail address:* L.Edwards@bham.ac.uk (L. Edwards).

0304-3959/$34.00 
doi:10.1016/j.pain.2007.10.010

cycle, in the normal physiological range, influence cortical processing of noxious stimuli. The current study investigated the influence of the cardiac cycle, as an index of pulsatile variations in blood pressure, on the cortical processing of nociception. The study used thulium-evoked laser stimulation, that exclusively activates nociceptive nerve fibers, to evoke pain-related late brain potentials [22,29]. Based on previous findings that the nociceptive flexion reflex is attenuated during systole, it was hypothesised that the N2–P2 amplitude, an objective index of the degree of induced pain [6], would be smaller during systole than diastole.

## 2. Methods

### 2.1. Participants

Ten healthy male normotensive volunteers, with a mean age of 33 years (SD = 6), mean height of 171 cm (SD = 4), mean weight of 65 kg (SD = 6), mean systolic blood pressure of 120 mmHg (SD = 11), mean diastolic blood pressure of 77 mmHg (SD = 9) and mean heart rate of 63 bpm (SD = 11), participated in the study. All participants were free from neurologic and psychiatric diseases and psychiatric and analgesic medications. Participants were asked to refrain from alcohol, caffeine and smoking for at least 12 h prior to testing. The study was approved by the Ethics Committee at National Institute for Physiological Sciences, Okazaki; all volunteers gave informed consent to participate.

### 2.2. Laser stimulation

A thulium:YAG laser stimulator (Carl Baasel Lasertech, Starnberg, Germany) was used to produce noxious stimuli. Laser pulses (1 ms in duration, 2000 nm in wavelength, and 3 mm in spot diameter) were delivered to the dorsum of the right hand at an interval of between 15 and 20 s. The irradiated points were moved slightly for each stimulus to avoid tissue damage and habituation of the receptors. At the start of the session, 10–20 laser stimuli were delivered to determine the stimulus intensity required to produce a painful sensation. After each stimulus, the participants rated the stimulus using a visual analogue scale (VAS), with anchors of 0 (no painful sensation) and 100 (imaginary intolerable pain sensation). A stimulus intensity ($M = 158$, SD = 9 mJ), rated as approximately 50 on the VAS, was used to examine pain-related evoked potentials (see below). At this laser intensity, all subjects rated the stimulus as a pricking pain sensation. Trained subjects can discriminate the first and second pain sensations, however, no subjects in this study reported a sensation other than pricking.

### 2.3. Laser evoked potential recording

The laser evoked potentials were recorded with an Ag/AgCl disk electrode placed over Cz (vertex), referred to the linked earlobes (A1 + A2) of the International 10/20 System. A pair of electrodes placed on the supra- and infra-orbit of the right eye was used for recording an electro-oculogram. An electrocardiogram was recorded using a pair of disk electrodes placed on each forearm. The impedance of all electrodes was kept below 5 kΩ. The electroencephalographic signals were recorded with a 0.1 to 100 Hz bandpass filter and digitized at a sampling rate of 1000 Hz. The period of analysis was 800 ms before to 600 ms after stimulus onset; the pre-stimulus period was used as the DC baseline. Individual trials containing artifacts due to eye blinks were rejected before averaging.

### 2.4. Procedure

Each subject was seated in an armchair in a quiet, electrically shielded, and temperature controlled (24 to 26 °C) room. Laboratory systolic blood pressure (mmHg), diastolic blood pressure (mmHg), and heart rate (bpm) were measured three times using a mercury sphygmomanometer and a brachial cuff attached to the participant's upper left arm. The experimental session consisted of 5 blocks of 12 trials. Each block was separated by a 10-min rest period. During the experiment, a fixation point (a white circle 2 cm in diameter) was displayed on a screen 1.5 m in front of the subjects from 10 to 15 s before until 2 s after each stimulus. Subjects were instructed to look at the fixation point when it was displayed. Two seconds after the onset of each stimulus, the fixation point disappeared and 'VAS' was displayed for 3 s, during which subjects rated the perceived sensation. Then the fixation point appeared again to prepare the next stimulus. The participants were instructed to rate the perceived pricking sensation associated with each laser stimulation by marking a 100 mm VAS.

### 2.5. Data reduction and analysis

The R-wave latency relative to stimulus onset (ms) and peak-to-peak amplitude (μV) of the N2–P2 component were measured in each trial. The peak of N2 and P2 was determined during a latency period of 180–240 and 280–400 ms, respectively, for each trial. To show the variability of N2/P2 components in each trial, the waveforms of 12 consecutive trials in a representative participant are depicted in Fig. 1. In addition, the amplitudes of each N2 and P2 component were measured, using a DC offset, from the prestimulus baseline of −100 ms to the peak negativity and positivity, respectively. Trials were then sorted into one of eight 100 ms wide intervals (each interval is labeled by its midpoint), whose minimum and maximum indicated the timing of the noxious stimulation after the R-wave: 0–99 ms (R + 50 ms), 100–199 ms (R + 150 ms), 200–299 ms (R + 250 ms), 300–399 ms (R + 350 ms), 400–499 ms (R + 450 ms), 500–599 ms (R + 550 ms), 600–699 ms (R + 650 ms) and 700–800 ms (R + 750 ms). The mean (SD) number of trials per R-wave to stimulation interval was 5.0 (1.6), 5.3 (2.8), 6.3 (2.8), 5.4 (2.8), 5.4 (1.8), 6.2 (1.9), 5.4 (2.9), 6.4 (2.2) for R-wave intervals R + 50 to R + 750 ms, respectively. All participants provided data for every R-wave to stimulation interval. Data were lost (25% of total number of trials) on trials with blink artifacts and trials when the R-wave occurred more than 800 ms before the onset of noxious stimulation. The mean N2, P2 and N2–P2 peak-to-peak amplitudes (μV) and pain ratings were calculated for each R-wave to stimulation interval. Repeated measures analyses of variance (ANOVAs) with R-wave to stimulation interval (i.e., R + 50,

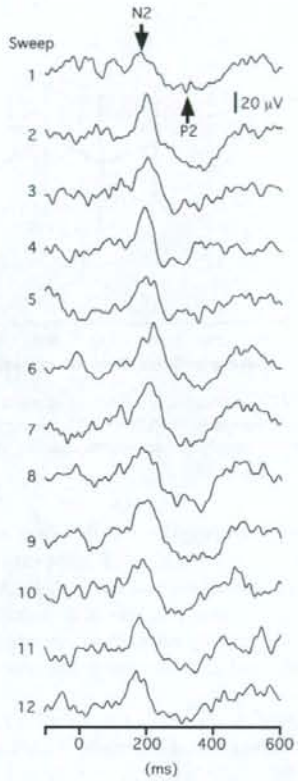


Fig. 1. Pain-related evoked potential waveforms of 12 consecutive trials, depicting N2 and P2, in a representative participant.

R + 150, R + 250, R + 350, R + 450, R + 550, R + 650, R + 750 ms) as a within-subjects factor were performed on the N2, P2 and N2–P2 amplitudes and pain ratings. ANOVAs were corrected for the assumption of independence of data points using the Huynh–Feldt correction ($\varepsilon$). Eta-squared ($\eta^2$), a measure of effect size, is also reported. A significance level of .05 was adopted. Significant results were followed by LSD post hoc tests. The data were analyzed using Statistica'99.

## 3. Results

### 3.1. N2–P2 peak-to-peak amplitudes

A repeated measures ANOVA (8 Intervals) revealed significant variations in the N2–P2 amplitude across the cardiac cycle, $\varepsilon = .74$, $F(7, 63) = 3.15$, $p = .02$, $\eta^2 = .26$, which were characterized by a quadratic trend, $F(1, 9) = 29.83$, $p = .0005$, $\eta^2 = .77$ (see Fig. 2). Post hoc comparisons confirmed that the N2–P2 amplitudes elicited by stimulation at R + 250, R + 350 and R + 450 ms were smaller than those elicited at R + 50, R + 150 and R + 750 ms. For illustrative purposes, the grand mean waveforms, averaged for the early (R + 50, R + 150 ms), middle (R + 250, R + 350, R + 450 ms) and late (R + 550, R + 650, R + 750 ms) phases of the cardiac cycle, are presented in Fig. 3, where it can be seen that the amplitudes were smaller mid-cycle compared to early and late cycle.

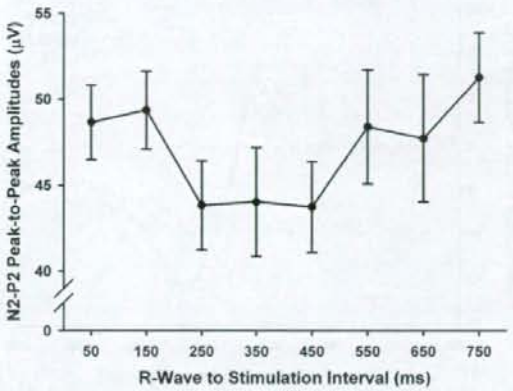


Fig. 2. Mean (SE) N2–P2 peak-to-peak amplitudes as a function of phase of the cardiac cycle. A repeated measures ANOVA revealed significant variations in the N2–P2 amplitude across the cardiac cycle ($p = .02$). Post hocs comparisons confirmed that N2–P2 amplitudes elicited by stimulation at R + 250, R + 350 and R + 450 ms were smaller than those elicited at R + 50, R + 150 and R + 750 ms. $N = 10$, Trials = 45. SE = SD ÷ $\sqrt{N}$.

### 3.2. N2 amplitudes

A repeated measures ANOVA (8 Intervals) revealed significant variations in the N2 amplitude across the cardiac cycle, $\varepsilon = .99$, $F(7, 63) = 4.13$, $p = .001$, $\eta^2 = .31$, which were characterized by a quadratic trend, $F(1, 9) = 25.43$, $p = < .001$, $\eta^2 = .74$ (see Fig. 4). Post hoc comparisons confirmed that the N2 amplitudes elicited by stimulation at R + 250 ms were smaller than those elicited at R + 50, R + 150, R + 650 and R + 750 ms. Stimulation at R + 350 ms produced smaller N2 amplitudes than R + 150, R + 650 and R + 750 ms. Finally, stimulation at R + 450 ms produced smaller N2 amplitudes than R + 650 and R + 750 ms.

### 3.3. P2 amplitudes

A repeated measures ANOVA (8 Intervals) did not reveal significant variations in the P2 amplitude across the cardiac cycle, $\varepsilon = .84$, $F(7, 63) = 0.73$, $p = .63$, $\eta^2 = .07$ (see Fig. 5).

### 3.4. Pain ratings

A repeated measures ANOVA (8 Intervals) revealed no significant differences in pain ratings across the cardiac cycle, $\varepsilon = .64$, $F(7, 63) = 1.10$, $p = .37$, $\eta^2 = .11$ (see Fig. 6).

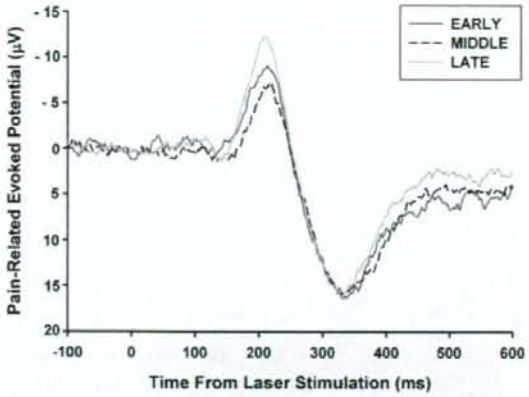


Fig. 3. Grand average pain-related evoked potentials waveforms grouped into early (R + 50 to R + 150 ms), middle (R + 250 to R + 450 ms), and late (R + 550 to R + 750 ms) phases of the cardiac cycle. $N = 10$, Trials = 45.

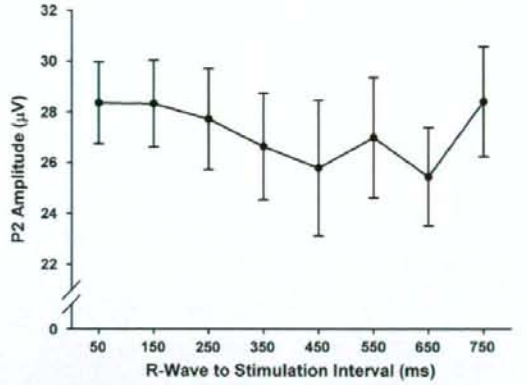


Fig. 5. Mean (SE) P2 amplitudes as a function of phase of the cardiac cycle. A repeated measures ANOVA did not reveal significant variations in the P2 amplitude across the cardiac cycle ($p = .63$). $N = 10$, Trials = 45. SE = SD + $\sqrt{N}$.

## 4. Discussion

The present study found significant variations across the cardiac cycle in the amplitude of the N2–P2 pain-related components of the evoked potential elicited by noxious laser stimulation. The N2–P2 amplitude difference is believed to be an objective index of the degree of induced pain [6]. Indeed, positive relationships have been found between the intensity of noxious laser stimuli, the amplitude of the N2–P2, and the magnitude of pain sensation [7]. The observation of smaller amplitude N2–P2 waveforms during the middle of the cardiac cycle indicates that pain-related cortical responses were attenuated during systole compared to diastole. Accordingly, these data support the hypothesis that stimulation of the arterial baroreceptors by natural changes in blood pressure during the cardiac cycle has a dampening effect on the nociceptive system.

In the present study, we only recorded the N2–P2 components of the evoked potential from one electrode at Cz. Therefore, the data cannot reveal the precise mechanisms of N2–P2 modulation across the cardiac cycle. However, the grand-averaged waveform (see Fig. 3) suggests that the cardiac cycle effect was larger for N2 than P2. Indeed, separate analyses of the N2

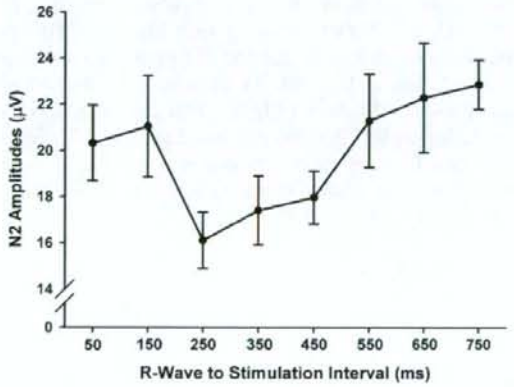


Fig. 4. Mean (SE) N2 amplitudes as a function of phase of the cardiac cycle. A repeated measures ANOVA revealed significant variations in N2 amplitude across the cardiac cycle, ($p = .001$). Post hocs comparisons confirmed that N2 amplitudes elicited by stimulation at R + 250 ms were smaller than those elicited at R + 50, R + 150, R + 650 and R + 750 ms. Stimulation at R + 350 ms produced smaller N2 amplitudes than R + 150, R + 650 and R + 750 ms. Finally, stimulation at R + 450 ms produced smaller N2 amplitudes than R + 650 and R + 750 ms. $N = 10$, Trials = 45. SE = SD + $\sqrt{N}$.

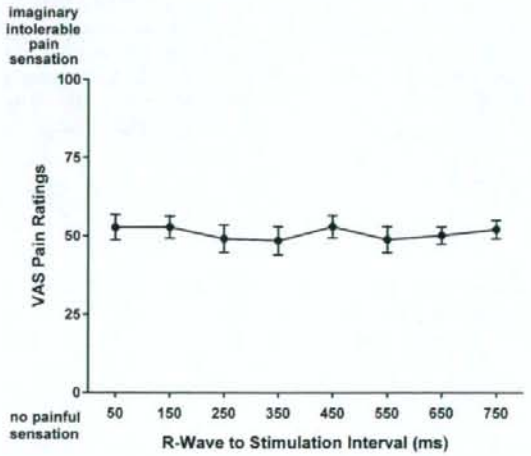


Fig. 6. Mean (SE) VAS pain ratings as a function of phase of the cardiac cycle. A repeated measures ANOVA revealed no significant differences in pain ratings across the cardiac cycle ($p = .37$). $N = 10$, Trials = 45. SE = SD + $\sqrt{N}$.

and P2 components revealed cardiac cycle time effects for N2 and not P2. The N2 and P2 components are generated mainly in the anterior cingulate cortex [8,43,46]. In addition to anterior cingulate cortex, the secondary somatosensory cortex or insula cortex contribute to shape the N2 component [8,31,43,46]. Therefore, our findings are compatible with the hypothesis that the target site of the interaction between N2 and P2 and baroreceptor output is the somatosensory or insula cortex. Further studies employing multi-channel recordings are required to test this hypothesis.

This is the first study, to our knowledge, to describe modulation of the pain-related evoked potential with natural variations in baroreceptor activation across the cardiac cycle. The current findings broadly agree with previous research which has reported reduced N2–P2 amplitudes elicited by intracutaneous stimulation of the finger during artificial stimulation of the baroreceptors using neck suction [3,28]. In addition, the current data are in line with reports of dampened lower limb nociceptive flexion reflex responding during systole compared to diastole [13–15,26]. The modulating effect of the cardiac cycle on the brain appears not to be exclusive to nociception. Auditory and visual perception vary with the phase of the cardiac cycle: sensitivity is generally lowest at the start of the cardiac cycle and increases as the cycle progresses [37,40]. Further, modulation of visual and auditory event-related potentials has been demonstrated during systole and diastole: the P1 component of the visual evoked potential [47] and the N1 component of the auditory evoked potential [38] were smaller during systole. Previous research has demonstrated that rhythmic oscillations of the EEG, most notably in the alpha range, were time locked to the carotid pressure wave [48]. Other research has examined the effects of artificial baroreceptor stimulation on the brain. A classic study in cats showed that mechanical stimulation of the carotid sinus baroreceptors had an inhibitory influence on cortical excitability [4]. Further, artificial baroreceptor stimulation in humans has been shown to cause a substantial reduction in slow cortical negative potentials, particularly the contingent negative variation, an index of cortical arousal [17,34,35]. Accordingly, the current cycle time effect for the pain-related evoked potential adds to a compelling body of evidence for a relationship between the cardiovascular system and the brain.

Pain was not modulated across the cardiac cycle in the current study. This is in line with previous studies which found no differences in pain reports for electrocutaneous stimuli delivered at various intervals after the R-wave of the electrocardiogram [13–15]. These findings contrast with the results of other studies that employed artificial baroreceptor manipulations. These studies reported that pain was lower during systole compared to diastole during neck suction [2], during repeated neck suction and compression [28,32], as well as during single neck suction and compression pulses [13]. These contradictory findings may be due to differences between natural and artificial baroreceptor stimulation studies in terms of the level of baroreceptor stimulation achieved.

The mechanism by which pain-related cortical processing is attenuated by the cardiac cycle has yet to be determined. However, it is reasonable to assume that these effects might be due to natural fluctuations in arterial baroreceptor activity across the cardiac cycle (see [15,16]). The integrated baroreceptor output of aortic baroreceptors located in the aortic arch and carotid sinus can be estimated to extend from 90 to 390 ms after the R-wave. The current study found that the N2–P2 amplitude was attenuated when noxious stimuli were delivered to the hand during the 200–299, 300–399 and 400–499 ms intervals after the R-wave. The onset latency of cortical activity in SI and SII, the proposed site of interaction, following noxious YAG laser stimulation to the hand has been recorded at 90–110 ms [30,49]. Thus, as N2–P2 was modulated from 200 ms after the R-wave, the earliest time the SII must be affected by baroreceptor activity is 290 ms after the R-wave. Accordingly, the observed pattern of modulation of the N2–P2 amplitude is compatible with the pattern of baroreceptor activation when a sensory transduction and processing delay of approximately 150 ms is included. This 150 ms delay may be explained by neural transmission times within the brainstem. For example, electrical stimulation of baroreceptor afferents in dogs and cats has been shown to cause inhibition of sympathetic activity with a latency of 150–200 ms, dependent on the recording site at the spinal level [10,36]. Allowing 10–15 ms for transmission of nerve impulses from carotid sinus and aortic arch to the nucleus of the solitary tract [42], and approximately 30 ms from the rostral ventrolateral medulla to sympathetic preganglionic neurons [25], this leaves 100–150 ms for transmission in the lower brainstem from the nucleus of the solitary tract to the rostral ventrolateral medulla [11]. This 100–150 ms transduction latency could perhaps explain the 150 ms delay between baroreceptor activation and attenuation of the N2–P2 amplitudes found in the current study. Further, there is substantial evidence suggesting that structures involved in the baroreflex pathway could also influence the pain system (for review, see [19]). For example, stimulation of the nucleus of the solitary tract induces antinociception [1] and the A5 cell group and locus coeruleus are sources of descending noradrenergic fibers that modulate spinal nociceptive transmission [27]. Furthermore, other evidence shows that pain areas are involved in baroreflex control. The periaqueductal grey matter, which produces analgesia when stimulated, can modulate the arterial baroreflex [21]. The nucleus raphe magnus in the rostral ventrolateral medulla, which plays a role in pain modulation, is involved in

the baroreflex pathway mentioned above, and also contains neurons that respond to noxious stimuli that show spontaneous fluctuations in phase with both natural variations and experimentally-induced changes in blood pressure [44,45]. Accordingly, this evidence demonstrates a close integration of areas involved in pain modulation and cardiovascular regulation.

The current study should be interpreted in light of some possible limitations. Neither blood pressure nor vessel diameter was measured during laser stimulation. Accordingly, the extent to which the pulse pressure wave distended the aortic arch and carotid sinus was not characterized, and therefore, the precise timing and magnitude of arterial baroreceptor stimulation is not known. Further, respiration was not measured in the current study and therefore the potential moderating effects of the phase of the respiratory cycle on the effects observed across the cardiac cycle were not determined. Given that baroreceptor function can vary between inspiration and expiration [12], research is needed to explore these putative effects. The sample size may be considered a potential weakness. However, many pain-related evoked potential studies tested similar numbers of participants. This study only tested men and therefore the generalizability of the cycle time effect for the N2–P2 amplitude needs to be determined in female participants. Accordingly, firm conclusions regarding the influence of baroreceptor activation on pain-related cortical processing should not be drawn until the current findings have been replicated by larger studies of mixed gender.

In conclusion, variations in the N2–P2 amplitudes across the cardiac cycle, with smaller amplitudes mid-cycle, indicated that cortical processing of nociception was attenuated during systole compared to diastole. These data support the hypothesis that arterial baroreceptors modulate the processing of nociception during each cardiac cycle.

## References


[1] Aicher SA, Randich A. Antinociception and cardiovascular responses produced by electrical stimulation in the nucleus tractus solitarius, nucleus reticularis ventralis, and the caudal medulla. Pain 1990;42:103–19.

[2] Al'Absi M, France CR, Ring C, France J, Harju A, McIntyre D, et al. Nociception and baroreceptor stimulation in hypertension-prone men and women. Psychophysiology 2005;42:83–91.

[3] Angrilli A, Mini A, Mucha RF, Rau H. The influence of low blood pressure and baroreceptor activity on pain responses. Physiol Behav 1997;62:391–7.

[4] Bonvallet M, Dell P, Hiebel G. Tonus sympathique et activite electrique corticale. Electroencephalogr Clin Neurophysiol 1954;6:119–44.

[5] Brody S, Angrilli A, Weiss U, Birbaumer N, Mini A, Veit R, et al. Somatotosensory evoked potentials during baroreceptor stimulation in chronic low back pain patients and normal controls. Int J Psychophysiol 1997;25:201–10.

[6] Bromm B, Lorenz J. Neurophysiological evaluation of pain. Electroencephalogr Clin Neurophysiol 1998;107:227–53.

[7] Bromm B. Laser-evoked cerebral potentials in the assessment of cutaneous pain sensitivity in normal subjects and patients. Rev Neurol 1991;147:625–43.

[8] Bromm B, Chen ACN. Brain electrical source analysis of laser evoked-potentials in response to painful trigeminal nerve-stimulation. Electroencephalogr Clin Neurophysiol 1995;95:14–26.

[9] Bromm B, Meier W. The intracutaneous stimulus – a new pain model for algesimetric studies. Methods Find Exp Clin Pharmacol 1984;6:405–10.

[10] Coote JH, Macleod VH, Fleetwoodwalker SM, Gilbey MP. Baroreceptor inhibition of sympathetic activity at a spinal site. Brain Res 1981;220:81–93.

[11] Dembowsky K, Mcallen RM. Baroreceptor inhibition of subretrofacial neurons – evidence from intracellular-recordings in the cat. Neurosci Lett 1990;111:139–43.

[12] Eckberg DL, Sleight P. Human baroreflexes in health and disease. Oxford: Clarendon Press; 1992.

[13] Edwards L, McIntyre D, Carroll D, Ring C, France CR, Martin U. Effects of artificial and natural baroreceptor stimulation on nociceptive responding and pain. Psychophysiology 2003;40:762–9.

[14] Edwards L, McIntyre D, Carroll D, Ring C, Martin U. The human nociceptive flexion reflex threshold is higher during systole than diastole. Psychophysiology 2002;39:678–81.

[15] Edwards L, Ring C, McIntyre D, Carroll D. Modulation of the human nociceptive flexion reflex across the cardiac cycle. Psychophysiology 2001;38:712–8.

[16] Edwards L, Ring C, McIntyre D, Carroll D, Martin U. Psychomotor speed in hypertension: effects of reaction time components, stimulus modality, and phase of the cardiac cycle. Psychophysiology 2007;44:459–68.

[17] Elbert T, Rockstroh B, Lutzenberger W, Kessler M, Pietrowsky R, Birbaumer N. Baroreceptor stimulation alters pain sensation depending on tonic blood pressure. Psychophysiology 1988;25:25–9.

[18] Gahery Y, Vigier D. Inhibitory effects in cuneate nucleus produced by vago-aortic afferent-fibers. Brain Res 1974;75:241–6.

[19] Ghione S. Hypertension-associated hypalgesia. Hypertension 1996;28:494–504.

[20] Handwerker HO, Kobal G. Psychophysiology of experimentally-induced pain. Physiol Rev 1993;73:639–71.

[21] Inui K, Murase S, Nosaka S. Facilitation of the arterial baroreflex by the ventrolateral part of the midbrain periaqueductal grey matter in rats. J Physiol 1994;477:89–101.

[22] Kakigi R, Shibasaki H, Ikeda A. Pain-related somatosensory evoked-potentials following $CO_2$-laser stimulation in man. Electroencephalogr Clin Neurophysiol 1989;74:139–46.

[23] Koch EB. Die Irradiation der pressorezeptorischen kreislaufreflexe. Klin Wochenschr 1932;2:225–7.

[24] Mancia G, Mark AL. Arterial baroreflexes in humans. In: Shepherd JT, Abboud FM, editors. Handbook of physiology. The cardiovascular system. Bethesda, Maryland: American Physiological Society; 1983. p. 755–93.

[25] Mcallen RM. Identification and properties of sub-retrofacial bulbospinal neurons – a descending cardiovascular pathway in the cat. J Auton Nerv Syst 1986;17:151–64.

[26] McIntyre D, Edwards L, Ring C, Parvin B, Carroll D. Systolic inhibition of nociceptive responding is moderated by arousal. Psychophysiology 2006;43:314–9.

[27] Miller JF, Proudfit HK. Antagonism of stimulation-produced antinociception from ventrolateral pontine sites by intrathecal administration of α-adrenergic antagonists and naloxone. Brain Res 1990;530:20–34.

[28] Mini A, Rau H, Montoya P, Palomba D, Birbaumer N. Baroreceptor cortical effects, emotions and pain. Int J Psychophysiol 1995;19:67–77.
[29] Mor J, Carmon A. Laser emitted radiant heat for pain research. Pain 1975;1:233–7.
[30] Nakata H, Inui K, Wasaka T, Tamura Y, Tran TD, Qiu YH, et al. Movements modulate cortical activities evoked by noxious stimulation. Pain 2004;107:91–8.
[31] Peyron R, Frot M, Schneider F, Garcia-Larrea L, Mertens P, Barral FG, et al. Role of operculoinsular cortices in human pain processing: converging evidence from PET, fMRI, dipole modeling, and intracerebral recordings of evoked potentials. Neuroimage 2002;17:1336–46.
[32] Rau H, Brody S, Larbig W, Pauli P, Vohringer M, Harsch B, et al. Effects of PRES baroreceptor stimulation on thermal an mechanical pain threshold in borderline hypertensives and normotensives. Psychophysiology 1994;31:480–5.
[33] Rau H, Elbert T. Psychophysiology of arterial baroreceptors and the etiology of hypertension. Biol Psychol 2001;57:179–201.
[34] Rau H, Elbert T, Lutzenberger W, Eves F, Rockstroh B, Larbig W, et al. Pavlovian conditioning of peripheral and central components of the baroreceptor reflex. J Psychophysiol 1988;2:119–27.
[35] Rau H, Pauli P, Brody S, Elbert T, Birbaumer N. Baroreceptor stimulation alters cortical activity. Psychophysiology 1993;30:322–5.
[36] Richter DW, Keck W, Seller H. Course of inhibition of sympathetic activity during various patterns of carotid sinus nerve stimulation. Pflugers Arch Eur J Physiol 1970;317:110–23.
[37] Sandman CA, McCanne TR, Kaiser DN, Diamond B. Heart rate and cardiac phase influence on visual perception. J Comp Physiol Psychol 1977;91:189–202.
[38] Sandman CA. Augmentation of the auditory event related potentials of the brain during diastole. Int J Psychophysiol 1984;2:111–9.
[39] Sandrini G, Serrao M, Rossi P, Romaniello A, Cruccu G, Willer JC. The lower limb flexion reflex in humans. Prog Neurobiol 2005;77:353–95.
[40] Saxon SA. Detection of near threshold signals during four phases of the cardiac cycle. Ala J Med Sci 1970;7:427–30.
[41] Scharein E, Bromm B. The intracutaneous pain model in the assessment of analgesic efficacy. Pain Rev 1998;5:216–46.
[42] Seller H, Illert M. Localization of first synapse in carotid sinus baroreceptor reflex pathway and its alteration of afferent input. Pflugers Arch Eur J Physiol 1969;306:1–19.
[43] Tarkka IM, Treede RD. Equivalent electrical source analysis of pain-related somatosensory-evoked potentials elicited by a Co2-Laser. J Clin Neurophysiol 1993;10:513–9.
[44] Thurston CL, Randich A. Effects of vagal afferent stimulation on ON and OFF cells in the rostroventral medulla: Relationships to nociception and arterial blood pressure. J Neurophysiol 1992;67:180–96.
[45] Thurston CL, Randich A. Responses to on and off cells in the rostral ventral medulla to stimulation of vagal afferents and changes in arterial pressure in intact and cardiopulmonary deafferentated rats. Pain 1995;62:19–38.
[46] Valeriani M, Rambaud L, Mauguiere F. Scalp topography and dipolar source modelling of potentials evoked by $CO_2$ laser stimulation of the hand evoked potentials. Electroencephalogr Clin Neurophysiol 1996;100:343–53.
[47] Walker BB, Sandman CA. Visual evoked potentials change as heart rate and carotid pressure change. Psychophysiology 1982;19:520–7.
[48] Walker BB, Walker JM. Phase relations between carotid pressure and ongoing electrocortical activity. Int J Psychophysiol 1983;1:65–73.
[49] Wang X, Inui K, Kakigi R. Early cortical activities evoked by noxious stimulation in humans. Exp Brain Res 2007;180:481–9.

# Neuromodulation

## Technology at the Neural Interface

VOLUME XI • NUMBER 1 • JANUARY 2008

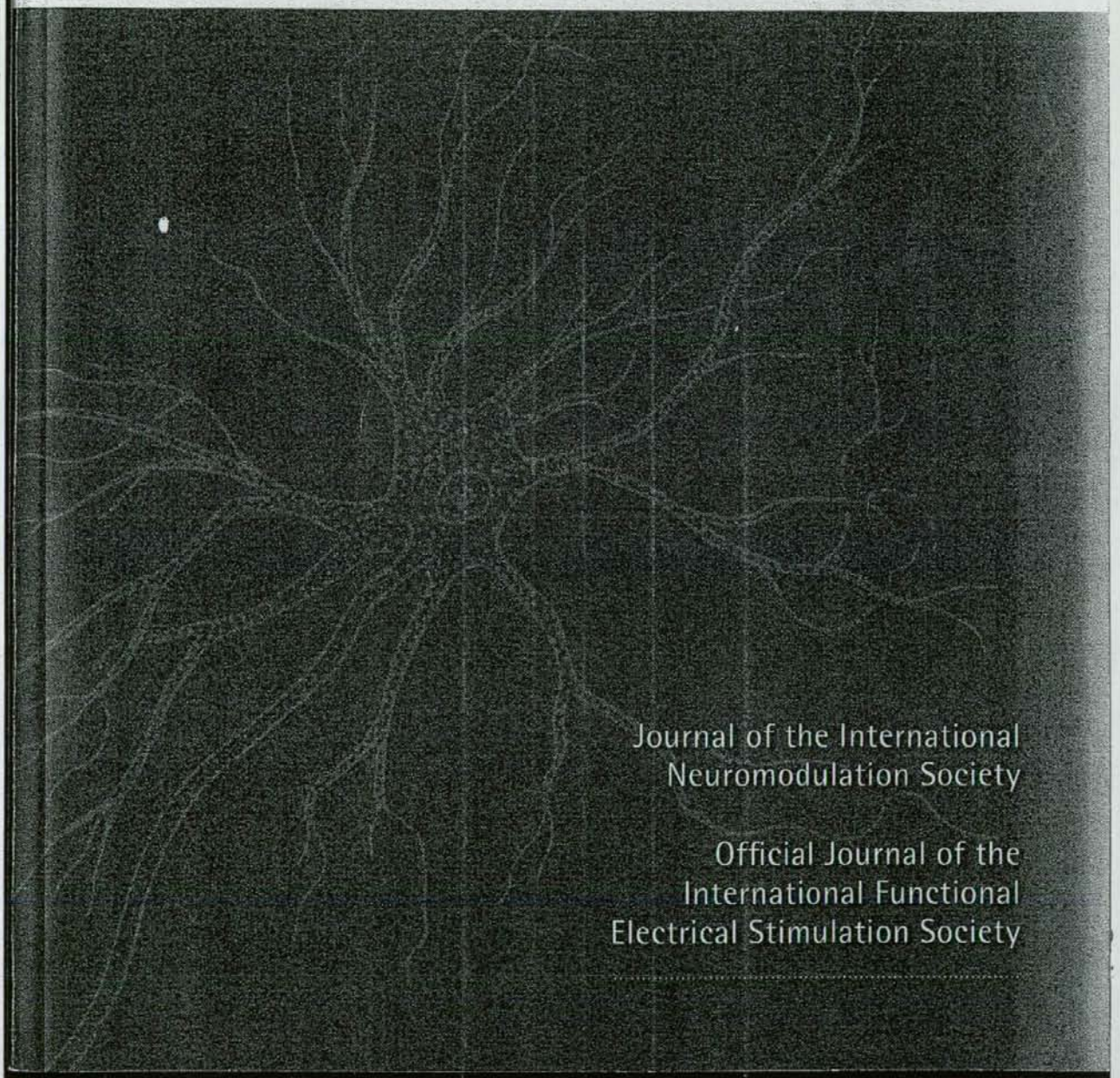

Journal of the International Neuromodulation Society

Official Journal of the International Functional Electrical Stimulation Society

NEUROMODULATION: TECHNOLOGY AT THE NEURAL INTERFACE

Volume 11 • Number 1 • 2008
http://www.blackwell-synergy.com/loi/ner

ORIGINAL ARTICLE

# Multiple-Cell Spike Density and Neural Noise Level Analysis by Semimicroelectrode Recording for Identification of the Subthalamic Nucleus During Surgery for Parkinson's Disease

Toshikazu Kano, MD, PhD[1,2] • Yoichi Katayama, MD, PhD[1,2] • Kazutaka Kobayashi, MD, PhD[1,2] • Masahiko Kasai, MD, PhD[1] • Hideki Oshima, MD, PhD[1] • Chikashi Fukaya, MD, PhD[1,2] • Takamitsu Yamamoto, MD, PhD[1,2]

*Department of Neurological Surgery, and Division of Applied System Neuroscience, Department of Advanced Medical Science, Nihon University School of Medicine, Tokyo, Japan*

## ABSTRACT

**Objective.** For targeting the subthalamic nucleus (STN), we attempted to quantify the changes in multiple cell activities by computing the neural noise level and multiple-cell spike density (MSD). **Methods.** We analyzed the neural noise level and MSD by stepwise recording at every 0.25-mm increment during the final tracking in 90 sides of 45 patients with Parkinson's disease. The MSD was analyzed with cut-off levels ranging from 1.2- to 2.0-fold the neural noise level in the internal capsule or zona incerta in each trajectory. **Results.** The dorsal boundary of the STN was identified from an increase in the neural noise ratio in all sides. The ventral boundary was identifiable, however, from a decrease in the neural noise ratio in only 70 sides (78%). In contrast, both the dorsal and ventral boundaries were clearly identified from an increase and a decrease in the MSD, respectively, in all of the 90 sides. **Conclusion.** MSD analysis by semimicroelectrode recording represents a useful, practical, and apparently reliable means for identifying the boundaries of the STN.

**KEY WORDS:** *Deep brain stimulation, Parkinson's disease, semimicroelectrode, subthalamic nucleus.*

## Introduction

Deep brain stimulation (DBS) of the subthalamic nucleus (STN) affords great benefits to the daily activity of patients with advanced Parkinson's disease (PD) (1–4). Most recent reports have placed emphasis on the microelectrode recording of single cell activity to refine the anatomical targeting of the STN during surgery (5–11). When the electrode has passed through the dorsal boundary of the STN, densely distributed cells characterized by irregular discharges are encountered (10,12,13). Detection of cells characterized by rapid and tonic discharges indicates that the electrode has passed through the dorsal boundary of the STN (14).

The ventral boundary of the STN, however, is sometimes unclear (10). This is because the cells in the STN

Submitted: July 10, 2007; accepted: September 11, 2007.
Address correspondence and reprint requests to: Yoichi Katayama, MD, PhD, Department of Neurological Surgery, Nihon University School of Medicine, 30-1 Ohyaguchi Kamimachi, Itabashi-ku, Tokyo 173-8610, JAPAN. Email: ykatayam@med.nihon-u.ac.jp

show several different discharge patterns (12,14). Multiple sampling of single cell activities is useful through changing the location of the electrode tip to determine whether or not the electrode has passed through the ventral boundary of the STN and entered the small band of white matter and pars reticulata of the substantia nigra (SNr).

We have been employing semimicroelectrode recording (1,15–18) for many years in an attempt to refine anatomical targeting. The semimicroelectrode can detect electrical events arising from a relatively wide area. This method results in stable recordings of spikes and neural noise generated by multiple cells at any location of the electrode tip, and enables stepwise recording with predetermined intervals. In addition, a relatively blunt tip of the semimicroelectrode, as compared to a sharp tip of the microelectrode, may be associated with a lower risk of hemorrhagic complications (14,19).

Semimicroelectrode recording of multiple cell activities as a whole reveals robust changes at the dorsal and ventral boundaries of the STN, and, therefore, appears to be more practical and time-saving. Little has yet been reported, however, concerning the standardization of such a technique. We attempted in the present study to quantify the changes in multiple cell activities by computing the multiple-cell spike density (MSD).

## Materials and Methods

### Patient Population

We analyzed data from intraoperative semimicroelectrode recordings in 45 patients, including 23 men and 22 women ranging in age from 42 to 80 (mean = 65), who underwent single-stage surgery for bilateral STN-DBS. These patients were diagnosed as having idiopathic PD and demonstrated past evidence of a good response to levodopa, but were disabled by severe motor symptoms despite receiving medications at a tolerable dose and schedule. The patients' Hoehn and Yahr stage with medication was within the range from stage III–V during the off-period, and stage II–IV during the on-period. The patients and their families gave informed consent for STN-DBS with intraoperative semimicroelectrode recording to be performed. Patients continued best medication on the day before the DBS operation and even on the morning of the day of the DBS operation. The clinical characteristics and demographic data for all 45 patients are summarized in Table 1.

**TABLE 1.** Clinical Characteristics and Demographic Data for All 45 Patients

| | Characteristics |
|---|---|
| No. of patients | 45 |
| Male/female ratio | 23:22 |
| Age (years)[a] | |
| At diagnosis | 55.3 ± 8.2 |
| At surgery | 65.0 ± 7.5 |
| LED (mg/day) | 627.0 ± 305.9 |
| UPDRS parts 1–4[a] | |
| On period | 39.3 ± 18.0 |
| Off period | 69.4 ± 20.9 |
| UPDRS part 3[a] | |
| On period | 21.7 ± 12.6 |
| Off period | 37.9 ± 14.5 |

[a]Data are expressed as the means ± SD.
LED, levodopa equivalent dose; UPDRS, Unified Parkinson's Disease Rating Scale.

### Surgical Procedures

A Leksell Series G head frame (Elekta Instrument AB, Stockholm, Sweden) was fixed to the skull. Magnetic resonance imaging (MRI; 1.5-tesla unit; Siemens Magnetom Vision®, Siemens AG, Erlangen, Germany) was carried out at a 1-mm slice thickness, and the anterior commissure and posterior commissure were identified with specialized software (Leksell SurgiPlan®, Elekta Instrument AB).

In an attempt to minimize cerebrospinal fluid leakage and, consequently, intraoperative brain shift, the head was elevated to approximately 30 degrees from the horizontal plane and the burr hole was made 30–35 mm anterior to the coronal suture and 20–25 mm lateral to the midline (17,20,21). The STN was then approached from the burr hole at an angle of 40–50 degrees to the horizontal plane parallel to the anterior commissure–posterior commissure line and 0–12.5 degrees to the sagittal plane. The tentative target was placed at the posteroventral boundary of the STN in such a way that the trajectory passed through the center of the STN. The trajectory was visualized three-dimensionally on MRI, onto which a digitized version of the Schaltenbrand-Wahren atlas (AtlasSpace®, Elekta Instrument AB) was superimposed (Fig. 1).

A DBS quadripolar electrode (model 3387; Medtronic Inc., Minneapolis, MN, USA) was placed through the frontal burr hole into the STN. Contact point 0 was placed in the posteroventral boundary of the STN, contact points 1 and 2 were placed within the STN, and contact point 3 was placed at the H fields of Forel or zona incerta (ZI) located just above the STN. Immediately after completion of the stereotactic operation, we undertook MRI again under conditions where the stereotactic frame was fixed to the skull, and the locations of each contact point of the DBS electrode were confirmed. The mean coordinates of the center of the most distal simulation point, as evaluated by postoperative MRI, were 11.0 mm lateral, 4.5 mm posterior, and 5.2 mm inferior to the mid-commissural point. DBS electrodes were implanted bilaterally as single-stage surgery in all patients. No hemorrhagic complications were encountered in this series of patients.



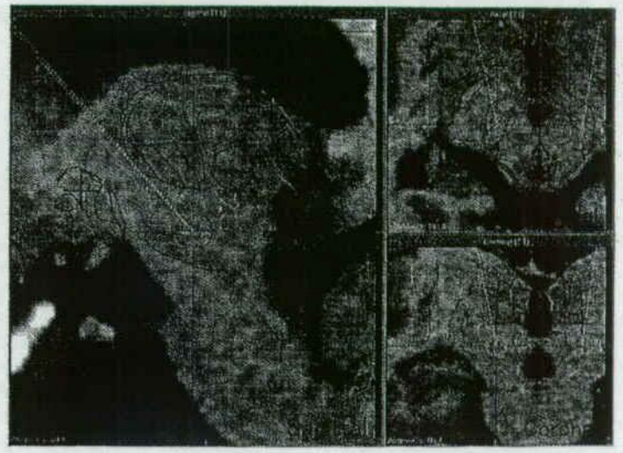

**FIGURE 1.** Simulation of the trajectory of the semimicroelectrode for targeting the STN. The trajectory is visualized three-dimensionally on MRI, onto which a digitized version of the Schaltenbrand–Wahren atlas adjusted to the size of each brain is superimposed. *Red crosses* indicate the positions of the anterior commissure and posterior commissure projected to the sagittal, axial, and coronal planes of the tentative target. *White dotted lines* indicate the simulated trajectory of the semimicroelectrode. *The green cross within a circle* is the tentative target, which is located at the posteroventral boundary of the STN. The simulated trajectory passes through the H2 fields of Forel (*yellow dotted triangle*) and the STN (*green dotted oval ring*). *The red dotted area* just below the tentative target is the SNr. MRI, magnetic resonance imaging; SNr, pars reticulata of the substantia nigra; STN, subthalamic nucleus.

### Semimicroelectrode Recording

Neural activities were recorded with a pencil-shaped bipolar concentric type semimicroelectrode (Unique Medical Co., Tokyo, Japan). The diameter of the exposed tip was approximately 0.1 mm, and the interpolar distance was 0.5 mm with an electrical resistance of 0.2 mΩ at 1000 Hz. The catheter needle (Leksell Stereotactic System, Elekta Instrument AB) with an outer diameter of 2.1 mm and inner diameter of 1.5 mm was first inserted and advanced to a point 10 mm above the tentative target, and the semimicroelectrode with a diameter of 1.0 mm was passed through the inside of the catheter needle.

Tracking with the semimicroelectrode was performed targeting the posteroventral boundary of the STN. The tip of the semimicroelectrode was advanced in consecutive 0.25-mm increments from a depth of 10 mm above the tentative target employing a hydraulic microdrive (Narishige Co., Tokyo, Japan). Recording first yielded the ventral anterior thalamic nucleus or the internal capsule (IC), and this was always followed by the ZI and H fields of Forel before entering the STN. In addition, the semimicroelectrode was further advanced 3 mm from the tentative target to confirm the border between the STN and the SNr. Signals were amplified, filtered (300 Hz to 10 kHz), displayed on an oscilloscope, played on an audio monitor, and stored in a data recorder. When the semimicroelectrode recording in the initial track failed to detect neural activity consistent with the STN at a length (distance from dorsal to ventral boundary) greater than 4 mm, a second tracking was made. We moved the tentative target depending on the characteristics of the recorded neural activity and the position of the semimicroelectrode verified from an intraoperative X-ray film taken after the semimicroelectrode recording.

### Analysis of Neural Noise Level and Multiple-Cell Spike Density

The electrical events recorded by a semimicroelectrode include spikes with variable amplitudes arising from multiple cells as well as neural noise, ie, fluctuations of field potentials generated by various neural elements. Large amplitude spikes could be separated from neural noise by setting an appropriate cut-off level of amplitude. It is not always possible, however, to separate small- or medium-sized spikes from sharp compound waves, which are contained in the neural noise. Therefore, we computed the density of spikes as well as sharp compound waves together, as the MSD, counting their occurrence at various cut-off levels.

In the final tracking by semimicroelectrode recording, we determined the neural noise level along the trajectory (Fig. 2A). The neural noise level was defined as the lowest cut-off level at which the neural noise was separated from larger amplitude spikes. The MSD at a given recording

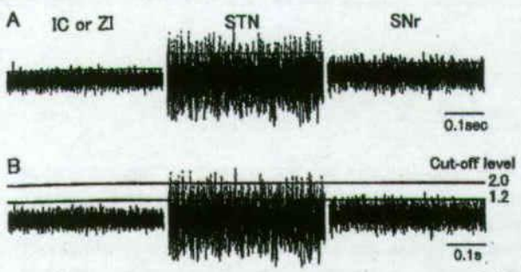


FIGURE 2. (A) Neural noise levels in the IC, STN and SNr. The neural noise level was defined as the lowest cut-off level at which the neural noise was separated from larger amplitude spikes. (B) Cut-off levels for analyzing the MSD were set in the range from 1.2- to 2.0-fold the neural noise level recorded at the IC or ZI. When the electrode entered the STN, the neural noise level was raised more than twofold the level recorded at the IC or ZI. IC, Internal capsule; MSD, multiple-cell spike density; SNr, pars reticulata of the substantia nigra; STN, subthalamic nucleus; ZI, zona incerta.

site was analyzed with cut-off levels ranging from 1.2- to 2.0-fold the neural noise level in the IC or ZI (Fig. 2B), and we examined to find the best cut-off level in each trajectory. Because, as the electrode enters the STN, the neural noise level is raised more than 2.0-fold the level in the IC or ZI (see Results), the MSD within the STN reflects both spikes and sharp compound waves, although spikes are predominantly represented at higher cut-off levels. For identification of the dorsal and ventral boundaries of the STN, the differences in neural noise level and MSD were compared at each 0.25-mm increment of the electrode. The neural noise level and MSD recorded at every 0.25-mm increment were averaged in each structure, and used for comparisons between the IC or ZI, the STN, and the SNr.

The data are expressed as the means ± standard deviation. For statistical analysis, the Mann–Whitney *U*-test was used for comparisons of the MSD and neural noise level, and the Kruskal–Wallis *H*-test for comparisons of the MSD within the STN. If the probability value was less than 0.05, the difference was considered to be significant. The present study was approved by the institutional committee for clinical research on humans.

## Results

### Changes in Neural Noise Level Along the Trajectory

The neural noise level clearly increased when the electrode crossed the dorsal boundary of the STN, and decreased when the electrode passed through the ventral boundary of the STN and entered the SNr (Fig. 3). The neural noise ratio (neural noise level in each structure/neural noise level in the IC or ZI) was clearly higher in the STN (2.52 ± 0.73) as compared to that of the SNr (1.43 ± 0.35; $p < 0.0001$, $N = 90$; Fig. 4).

The dorsal boundary of the STN was definitely identified from an increase in neural noise ratio during the final tracking in all of the 90 sides. The ventral boundary of the STN was identifiable, however, from a decrease in neural noise ratio during the final tracking in only 70 (78%) of the 90 sides. In the remaining 20 sides (22%), the border between the STN and SNr was unclear (Fig. 5A). In these cases, the neural noise ratio began to decrease in the posteroventral part of the STN before the electrode passed through the ventral boundary of the STN as presumed by MSD analysis (see below).

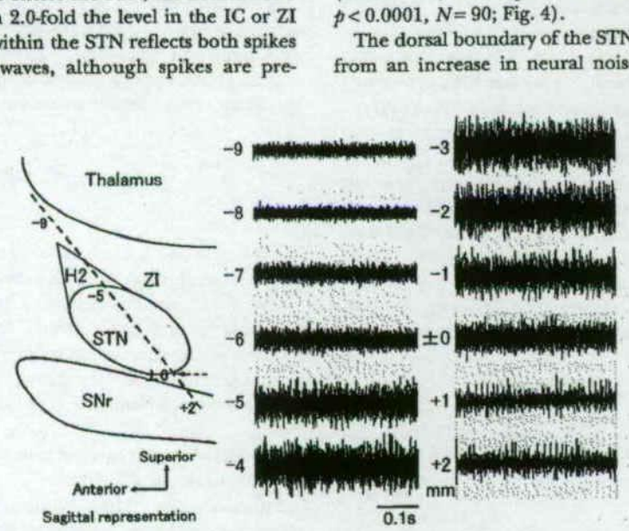


FIGURE 3. Changes in multiple cell activities along the trajectory (*dotted line*) passing through the subthalamic nucleus (STN). The recording, which was initiated at 10 mm above the tentative target, first yielded the internal capsule, followed by the zona incerta (ZI) and H2 field of Forel (H2), STN, and substantia nigra (SNr). The multiple cell activities increased markedly when the electrode entered the STN, and decreased when the electrode passed through the ventral boundary of the STN. Numbers indicate the distance (mm) from the tentative target (*dotted arrow*) set at the posteroventral boundary of the STN.



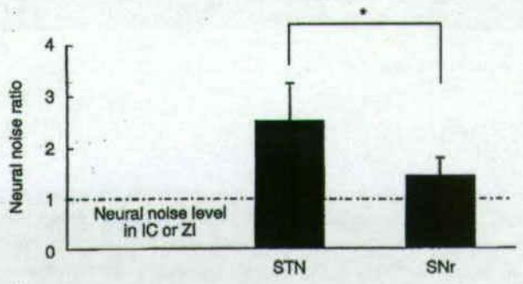


FIGURE 4. Comparison of neural noise levels along the trajectory passing through the STN. Data are expressed as the neural noise ratio (neural noise level in each structure/neural noise level in the IC or ZI), $*p < 0.0001$. IC, internal capsule; STN, subthalamic nucleus; ZI, zona incerta.

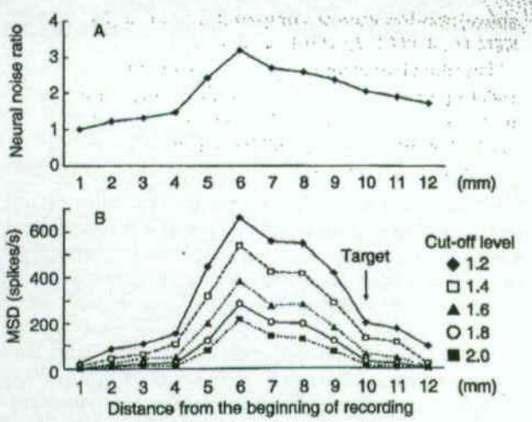


FIGURE 5. (A) Representative example of changes in neural noise level in the STN and SNr. (B) Changes of MSD in the STN and SNr at different cut-off levels in the same case as shown in A. The cut-off level was varied from 1.2- to 2.0-fold the neural noise level in the IC. The MSD increased at 5 mm from the point where the recording was initiated, and decreased at the tentative target point (10 mm). A cutoff level of 1.2-fold revealed the clearest changes. IC, internal capsule; MSD, multiple-cell spike density; SNr, pars reticulata of the substantia nigra; STN, subthalamic nucleus.

### Change in Multiple-Cell Spike Density Along the Trajectory

The MSD clearly increased when the electrode crossed the dorsal boundary of the STN, and decreased when the electrode passed through the ventral boundary of the STN and entered the SNr. The MSD within the STN was large as compared to that in the IC or ZI and that in the SNr at any cut-off level ranging from 1.2- to 2.0-fold (Fig. 5B). The cut-off level of 1.2-fold revealed the largest increase in MSD in the STN (554 ± 201 spikes/s), which was markedly higher than the MSD in the IC or ZI (19 ± 11 spikes/s; $p < 0.0001$, $N = 90$) and SNr (106 ± 77 spikes/s; $p < 0.0001$, $N = 90$) at this cut-off level. The dorsal and ventral boundaries of the STN were clearly identified from the increase and decrease in the MSD, respectively, in all of the 90 sides.

Along the trajectory of the semimicroelectrode, we divided the STN into 4 parts equally, and named them sequentially as part 1 to part 4 in the direction from the most anterodorsal part (part 1) to the most posteroventral part (part 4). The MSD was the lowest in part 4 (404 ± 130 spikes/s) as compared to part 1 (560 ± 185 spikes/s; $p < 0.0001$, $N = 90$), part 2 (601 ± 226 spikes/s; $p < 0.0001$, $N = 90$) and part 3 (543 ± 205 spikes/s; $p < 0.0001$, $N = 90$; Fig. 6). Nevertheless, the MSD in the SNr (see

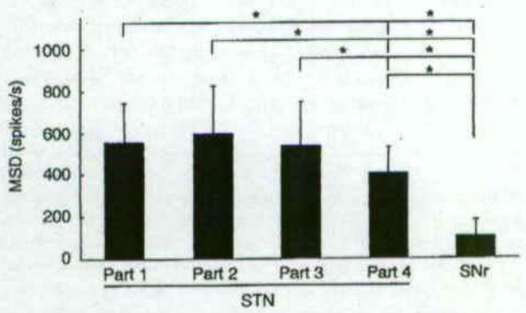


FIGURE 6. Changes in MSD within the STN and SNr. The trajectory passing through the STN was divided equally into 4 parts. The parts were named in such a way that the most anterodorsal part of the STN was part 1, and the most posteroventral part of the STN was part 4. The MSD was lower in part 4 as compared to any of the other parts. The MSD in the SNr was the lowest, as compared to any of the four parts within the STN, $*p < 0.0001$. MSD, Multiple-cell spike density; SNr, pars reticulata of the substantia nigra; STN, subthalamic nucleus.

above) was low even as compared to that of part 4 of the STN ($p < 0.0001$, $N = 90$).

The initial tracking correctly targeted the STN in 40 (88.9%) of the 45 initially operated sides (number of trackings, $1.1 \pm 0.4$; length of the STN at final tracking, $6.0 \pm 1.2$ mm) and in 42 (93.3%) of the 45 contralateral sides (number of trackings, $1.1 \pm 0.3$; length of the STN at final tracking, $5.8 \pm 1.1$ mm). Two or more trackings were needed in the remaining sides. In total, 82 (91.1%) of the 90 initial trackings correctly targeted the STN (number of trackings, $1.1 \pm 0.3$).

## Discussion

### Dorsal Boundary of the Subthalamic Nucleus

The present study demonstrated that the neural noise level and MSD clearly increased when the electrode entered the STN. Hutchison et al. (12) reported that when the microelectrode entered the STN, cells generating large amplitude spikes were encountered. In the typical recording within the STN reported by Starr et al. (10), large amplitude spikes from multiple cells and elevated neural noise levels can be seen. The increases in neural noise level and MSD at the dorsal boundary of the STN are consistent with these findings. It appears that the neural noise level and MSD reflect the discharge rate of multiple cells on average and the cell density.

The present study also revealed that the neural noise level in some cases decreased gradually in the posteroventral part of the STN. In addition, the MSD was lower in this part as compared to the rest of the STN. It has been reported that the cellularity of the STN is homogenous in the monkey (22). Sterio et al. (23) found by microelectrode recording, however, that the cell density, estimated from the encountered single cell activity, was lower in the ventral part of the STN ($4.7 \pm 1.8$ cells/mm) as compared to the dorsal part of the STN ($6.8 \pm 2.0$ cells/mm), and the discharge rate of cells was lower in the ventral part of the STN ($43 \pm 9.5$ Hz) as compared to the dorsal part of the STN ($52 \pm 12$ Hz). The gradual decrease in neural noise and relatively lower MSD in the posteroventral part of the STN are consistent with these findings, again indicating that they efficiently reflect both the discharge rate of multiple cells on average and the cell density.

### Ventral Boundary of the Subthalamic Nucleus

The discharge rate of STN cells is approximately half the discharge rate of SNr cells, if analyzed as the single cell activity by microelectrode recordings. Hutchison et al. (12) reported that while STN cells show discharges with an irregular pattern at varying rates ranging from 25 to 45 Hz ($37 \pm 17$ Hz), SNr cells exhibit discharges with a more regular pattern at a much faster rate ($71 \pm 23$ Hz). The illustration in their report indicates that the background multiple cell activities are higher in the SNr than in the STN. Starr et al. (10) also reported that cells in the SNr showed discharges at a faster rate ($86 \pm 16$ Hz) as compared to cells in the STN ($34 \pm 14$ Hz).

In contrast to these previous data obtained by microelectrode recording, the neural noise level and MSD were always higher in the STN than in the SNr in the present study. The background multiple cell activities may vary in microelectrode recording depending on the location of the electrode tip. The discrepancy in spike density (discharge rate) between studies employing microelectrodes and semimicroelectrodes appears to reflect a difference in the capability of detecting information regarding the cell density in addition to the discharge rate of cells on average.

### Targeting by Semimicroelectrode Recording

The present results demonstrated that the ventral boundary was not always identifiable from the neural noise level alone, because it begins to decrease in the posteroventral part of the STN. In contrast, the dorsal and ventral boundaries of the STN were always identified by MSD analysis with appropriate tracking, indicating that MSD analysis is more important for determining the boundaries of the STN. Although there was no anatomical verification, these functionally defined boundaries represent the most important information for appropriate placement of the DBS electrode within the STN.

In the present study, the lowest cut-off level of 1.2-fold revealed the largest changes. This is clearly because the MSD at such a cut-off level includes fluctuations of the field potential that becomes larger in amplitude within the STN. Because the increase in amplitude of the field potential may also reflect an increase in multiple cell activities as well as the cell density, the significance of MSD analysis may not differ at any cut-off level for determining the boundaries of the STN.

It has been reported that detection of movement-related cells is important for the identification of the dorsolateral part of the STN, and the DBS electrode should be placed in this region (11,14,24). It is not readily possible to isolate such cells with a semimicroelectrode, which may be the only major drawback of the use of a semimicroelectrode.

If the DBS electrode is placed too lateral, however, the stimulation current may spread to the corticospinal tract. We therefore examined by stimulation whether or not the electrode is too close to the lateral boundary of the STN. The distance of the DBS electrode from the midline, as measured on postoperative MRI (see Materials and Methods), in the present series of patients was the same as the distance reported previously by others (11–12 mm) (8,10).

## Conclusion

The present study suggests that MSD analysis by semimicroelectrode recording represents a useful, practical, and apparently reliable means for identifying the boundaries of the STN.



## Acknowledgments

This work was supported by Grants-in-Aid for Scientific Research from the Ministry of Education, Culture, Sports, Science, and Technology, Japan (Nos. A12307029 and A15209047), Technology for the promotion of the industry-university collaboration at Nihon University, Japan, and a Program Grant from the Ministry of Health, Labor, and Welfare, Japan.

## References

1. Katayama Y, Kasai M, Oshima H et al. Subthalamic nucleus stimulation for Parkinson's disease: benefits observed in levodopa-intolerant patients. *J Neurosurg* 2001;95:213–221.
2. Krack P, Batir A, Van Blercom N et al. Five-year follow-up of bilateral stimulation of the subthalamic nucleus in advanced Parkinson's disease. *N Engl J Med* 2003;349:1925–1934.
3. Limousin P, Krack P, Pollak P et al. Electrical stimulation of the subthalamic nucleus in advanced Parkinson's disease. *N Engl J Med* 1998;339:1105–1111.
4. The Deep-Brain Stimulation for Parkinsonís Disease Study Group. Deep-brain stimulation of the subthalamic nucleus or the pars interna of the globus pallidus in Parkinson's disease. *N Engl J Med* 2001;345:956–963.
5. Abosch A, Hutchison WD, Saint-Cyr JA, Dostrovsky JO, Lozano AM. Movement-related neurons of the subthalamic nucleus in patients with Parkinson's disease. *J Neurosurg* 2002;97:1167–1172.
6. Cuny E, Guehl D, Burbaud P, Gross C, Dousset V, Rougier A. Lack of agreement between direct magnetic resonance imaging and statistical determination of a subthalamic target: the role of electrophysiological guidance. *J Neurosurg* 2002;97:591–597.
7. Guridi J, Rodriguez-Oroz MC, Lozano AM et al. Targeting the basal ganglia for deep brain stimulation in Parkinson's disease. *Neurology* 2000;55 (Suppl. 6):S21–S28.
8. Hamid NA, Mitchell RD, Mocroft P, Westby GW, Milner J, Pall H. Targeting the subthalamic nucleus for deep brain stimulation. Technical approach and fusion of pre- and postoperative MR images to define accuracy of lead placement. *J Neurol Neurosurg Psychiatry* 2005;76:409–414.
9. Priori A, Egidi M, Pesenti A et al. Do intraoperative microrecordings improve subthalamic nucleus targeting in stereotactic neurosurgery for Parkinson's disease? *J Neurosurg Sci* 2003;47:56–60.
10. Starr PA, Christine CW, Theodosopoulos PV et al. Implantation of deep brain stimulators into the subthalamic nucleus: technical approach and magnetic resonance imaging-verified lead locations. *J Neurosurg* 2002;97:370–387.
11. Starr PA, Vitek JL, DeLong M, Bakay RA. Magnetic resonance imaging-based stereotactic localization of the globus pallidus and subthalamic nucleus. *Neurosurgery* 1999;44:303–313.
12. Hutchison WD, Allan RJ, Opitz H et al. Neurophysiological identification of the subthalamic nucleus in surgery for Parkinson's disease. *Ann Neurol* 1998;44:622–628.
13. Zonenshayn M, Rezai AR, Mogilner AY, Beric A, Sterio D, Kelly PJ. Comparison of anatomic and neurophysiological methods for subthalamic nucleus targeting. *Neurosurgery* 2000;47:282–292.
14. Rodriguez-Oroz MC, Rodriguez M, Guridi J et al. The subthalamic nucleus in Parkinson's disease: somatotopic organization and physiological characteristics. *Brain* 2001;124:1777–1790.
15. Lanotte MM, Rizzone M, Bergamasco B, Faccani G, Melcarne A, Lopiano L. Deep brain stimulation of the subthalamic nucleus, anatomical, neurophysiological, and outcome correlations with the effects of stimulation. *J Neurol Neurosurg Psychiatry* 2002;72:53–58.
16. Lopez-Flores G, Miguel-Morales J, Teijciro-Amador J et al. Anatomic and neurophysiological methods for the targeting and lesioning of the subthalamic nucleus: Cuban experience and review. *Neurosurgery* 2003;52:817–830.
17. Yamamoto T, Katayama Y, Fukaya C, Oshima H, Kasai M, Kobayashi K. New method of deep brain stimulation therapy with two electrodes implanted in parallel and side by side. *J Neurosurg* 2001;95:1075–1078.
18. Yokoyama T, Sugiyama K, Nishizawa S et al. Neural activity of the subthalamic nucleus in Parkinson's disease patients. *Acta Neurochir (Wien)* 1998;140:1287–1290.
19. Binder DK, Rau G, Starr PA. Hemorrhagic complications of microelectrode-guided deep brain stimulation. *Stereotact Funct Neurosurg* 2003;80:28–31.
20. Yamamoto T, Katayama Y, Kano T, Kobayashi K, Oshima H, Fukaya C. Deep brain stimulation for the treatment of parkinsonian, essential, and poststroke tremor: a suitable stimulation method and changes in effective stimulation intensity. *J Neurosurg* 2004;101:201–209.
21. Yamamoto T, Katayama Y, Kobayashi K, Oshima H, Fukaya C. Dual-floor burr hole adjusted to burr-hole ring and cap for implantation of stimulation electrodes. *J Neurosurg* 2003;99:783–784.
22. Parent A, Hazrati LN. Functional anatomy of the basal ganglia. II. The place of subthalamic nucleus and external pallidum in basal ganglia circuitry. *Brain Res Brain Res Rev* 1995;20:128–154.
23. Sterio D, Zonenshayn M, Mogilner AY et al. Neurophysiological refinement of subthalamic nucleus targeting. *Neurosurgery* 2002;50:58–67.
24. Romanelli P, Heit G, Hill BC, Kraus A, Hastie T, Bronte-Stewart HM. Microelectrode recording revealing a somatotopic body map in the subthalamic nucleus in humans with Parkinson's disease. *J Neurosurg* 2004;100:611–618.

*Reprinted from*

*Journal of Neurosurgery*

# Direct inhibition of levodopa-induced beginning-of-dose motor deterioration by subthalamic nucleus stimulation in a patient with Parkinson disease

Case report

HIDEKI OSHIMA, M.D., PH.D., YOICHI KATAYAMA, M.D., PH.D., CHIKASHI FUKAYA, M.D., PH.D., TOSHIKAZU KANO, M.D., KAZUTAKA KOBAYASHI, M.D., PH.D., TAKAMITSU YAMAMOTO, M.D., PH.D., AND YUTAKA SUZUKI, M.D., PH.D.

**JANUARY 2008** Volume 108, Number 1:160-163



American Association of Neurological Surgeons

**WWW.THEJNS.ORG**

J Neurosurg 108:160–163, 2008

# Direct inhibition of levodopa-induced beginning-of-dose motor deterioration by subthalamic nucleus stimulation in a patient with Parkinson disease

## Case report

Hideki Oshima, M.D., Ph.D.,[1,2] Yoichi Katayama, M.D., Ph.D.,[1,2] Chikashi Fukaya, M.D., Ph.D.,[1,2] Toshikazu Kano, M.D.,[2] Kazutaka Kobayashi, M.D., Ph.D.,[2] Takamitsu Yamamoto, M.D., Ph.D.,[1,2] and Yutaka Suzuki, M.D., Ph.D.[1,3]

*[1]Division of Applied System Neuroscience, and Departments of [2]Neurological Surgery and [3]Neurology, Nihon University School of Medicine, Tokyo, Japan*

✓Beginning-of-dose motor deterioration (BDMD) is a complication of levodopa medications in Parkinson disease (PD) that is presumably caused by inhibitory effects of levodopa. Only limited experience of BDMD has been described in the literature. The authors report the case of a patient with PD who demonstrated a marked BDMD while being treated with standard levodopa medications. This 55-year-old woman had a 12-year history of PD and a 10-year history of levodopa treatment. Marked exacerbation of symptoms occurred 15 to 20 minutes after every dose of levodopa at 100 mg and lasted approximately 15 minutes. The PD symptoms, particularly tremor and rigidity, were exacerbated more markedly during this period than during the wearing-off deterioration. The BDMD could be controlled very well by subthalamic nucleus (STN) stimulation without any change in the regimen of levodopa medications. These observations suggest that the BDMD was inhibited by STN stimulation through a direct effect.
*(DOI: 10.3171/JNS/2008/108/01/0160)*

**Key Words** • **deep brain stimulation** • **inhibitory effect** • **levodopa** • **motor fluctuation** • **Parkinson disease** • **subthalamic nucleus**

On-off fluctuation of motor symptoms, which follows exposure to chronic, repetitive administration of levodopa medications, often complicates levodopa therapy in patients with advanced PD. End-of-dose or "wearing-off" motor deterioration parallels the fall in plasma concentration of levodopa.[3,17] In addition, end-of-dose motor deterioration caused by inhibitory effects of levodopa plunges patients into a worsening of disability from their baseline off-medication motor status.[2,16] In 1992, Merello and Lees[12] first reported that some patients with PD also demonstrate motor deterioration, presumably through similar inhibitory effects of levodopa on the rising phase of the plasma levodopa concentration.[6,11–13,16] This phenomenon was designated as "beginning-of-dose motor deterioration,"[12] abbreviated in the present paper as BDMD.

Stimulation of the STN can ameliorate on-off motor fluctuations,[1,4,8–10,14] by attenuating the wearing-off motor deterioration.[18] This effect of STN stimulation is similar to the effects of a maximal dose of levodopa in each patient.[1,4,8,9,14,18] In contrast, little is yet known regarding the influence of STN stimulation on the motor deterioration caused by inhibitory effects of levodopa. We report on a patient with PD who demonstrated a marked BDMD under standard levodopa medications, which was found to be inhibited directly by STN stimulation withstanding levodopa medications.

*Abbreviations used in this paper:* BDMD = beginning-of-dose motor deterioration; PD = Parkinson disease; STN = subthalamic nucleus; UPDRS = Unified Parkinson's Disease Rating Scale.

### Case Report

*History and Presentation.* This 55-year-old woman had a 12-year history of PD and a 10-year history of levodopa treatment. Although her PD symptoms had progressively worsened, she was being treated with a restricted dose of levodopa because of levodopa-induced hallucinations: 400/40 mg levodopa/dopa-decarboxylase (100/10 mg four times daily), 750 μg pergolide mesylate (250 μg three times daily), and 10 mg selegiline hydrochloride per day. She eventually developed medically uncontrollable on-off motor fluctuations and came to experience BDMD as well as levodopa-induced dose-onset dyskinesia. For these reasons, she was referred to us for STN stimulation.





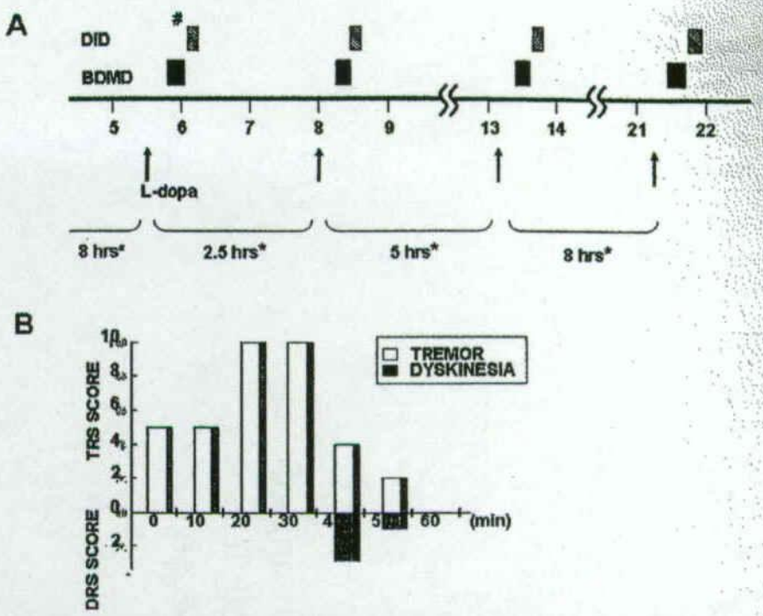


Fig. 1. A: Graph showing the temporal relationship between BDMD and dose-onset dyskinesia (DID) in a patient with PD after administration of levodopa (L-dopa). The *asterisks* indicate intervals from the previous dose of levodopa in hours. B: Temporal relationship between the appearance of tremor in BDMD and dose-onset dyskinesia after an early-morning levodopa dose (indicated by *number sign* in A). DRS = dyskinesia rating scale; TRS = tremor rating scale.

When the patient presented to us the total duration of the off-medication period reached 50% of the day. She complained that the BDMD always appeared after every dose of levodopa.

*Presurgical Evaluation.* During 2 days of observation, we confirmed that the BDMD occurred at 15 to 20 minutes after every dose of levodopa at 100 mg and lasted for approximately 15 minutes, while the intervals from the previous dose of levodopa varied in the range from 2.5 to 8 hours (Fig. 1). The severity of the BDMD was variable, and the BDMD after the first dose of levodopa in the early morning was apparently most severe (Fig. 1B, Table 1). Exacerbation of the PD symptoms, particularly the tremor and rigidity, which predominated in the lower extremities, was noticeably worse during the BDMD than during the wearing-off period. The motor (Part III) score on the UPDRS was increased during the BDMD by 188% from the score during the best on-medication motor condition (on period) and by 44% from the score during the wearing-off motor deterioration (off period). The BDMD was followed by levodopa-induced dose-onset dyskinesia, which consisted of dystonic posture and pain in the left lower extremity (Fig. 1). The temporal relationship between the BDMD and dyskinesia was uniform, the onset and peak of the BDMD always preceded those of the dyskinesia by 15 to 20 minutes. These clinical findings were consistent with the characteristics of BDMD described in the literature.[12] It was impossible to attribute such short-lived motor deterioration to a continuation of wearing-off or end-of-dose motor deteriorations, since it occurred abruptly and invariably after every dose of levodopa, despite varying intervals between doses.

*Surgery and Postsurgical Course.* The patient underwent implantation of electrodes (Model 3387, Medtronic, Inc.) and pulse generators for deep brain stimulation of the STN bilaterally. The PD symptoms were greatly improved by bipolar STN stimulation, especially during the off periods, at intensities ranging from 2.0 to 2.5 V (pulse width 180 μsec, frequency 135 Hz) during the follow-up period. Subsequent to the initiation of STN stimulation, the doses of medication were reduced to 200/20 mg levodopa/dopa-decarboxylase, 750 μg pergolide mesylate, and 10 mg selegiline hydrochloride per day. The medications were not completely withdrawn, because the patient reported some motor deterioration in the afternoon (lasting approximately 30 minutes). We confirmed that the BDMD was still induced by every dose of levodopa at 100 mg if the STN stimulation was kept turned off, and was immediately attenuated when the STN stimulation was turned on at intensities of $> 1.8$ V. Complete inhibition of the BDMD was achieved at intensities of $> 2.5$ V.

Standard follow-up evaluation at 6 months after surgery revealed that the UPDRS motor score was markedly improved by bilateral STN stimulation at an intensity of 2.0 V during the off period as well as the on period (78 and 75%, respectively; Table 1). The dose-onset dyskinesia disappeared completely. The BDMD was controlled almost com-

TABLE 1

*Preoperative and postoperative UPDRS scores**

| UPDRS Measure (max score) | Preop | | | Postop (% impr‡) | | |
|---|---|---|---|---|---|---|
| | | Off | | 6 Mos | | |
| | On | WO | BDMD (% deter†) | On | Off | 12 Mos§ |
| ADL (52) | 3 | 17 | 19 (12) | 2 (33) | 5 (74) | 2 |
| motor (108) | 16 | 32 | 46 (44) | 4 (75) | 10 (78) | 5 |
| tremor (20) | 0 | 5 | 10 (100) | 0 | 2 (80) | 0 |
| rigidity (20) | 5 | 8 | 12 (50) | 1 (80) | 1 (92) | 1 |
| akinesia (32) | 7 | 11 | 13 (18) | 0 (100) | 2 (85) | 1 |
| posture (8) | 0 | 2 | 2 (0) | 0 | 1 (50) | 0 |
| gait (4) | 0 | 1 | 2 (50) | 0 | 0 (100) | 0 |

* ADL = activity of daily living; deter = deterioration; impr = improvement; Off = off period; On = on period; WO = wearing-off period.
† Percentage deterioration compared with wearing-off.
‡ Percentage improvement compared with before surgery.
§ No off-medication assessment was performed at the 12-month follow-up evaluation because a "no off-medication" condition had been achieved.

pletely, leaving occasional slight and transient tremor in the lower extremities. The results of this evaluation confirmed that the immediate effect of STN stimulation on the BDMD had remained unchanged. The improvement had lasted and a "no off-medication" motor condition had been achieved at 12 months after surgery. We attempted a dopa challenge test (100 mg/10 mg levodopa/dopa-decarboxylase administered orally) at 14 months postoperatively, but BDMD did not occur.

## Discussion

Merello and Lees[12] reported BDMD occurring at 10 to 20 minutes after intake of levodopa and lasting for 10 to 20 minutes. Before their report, this phenomenon had been regarded as part of wearing-off or end-of-dose motor deterioration that continued until the next dose of levodopa.[3,16]

Although it has been suggested that BDMD might be common,[12] only limited experience of it has been described in the literature.[6,11–13,16] It appears possible that BDMD can be confused with coexisting levodopa-induced dose-onset dyskinesia.[12] In addition, most cases of BDMD have been detected previously under intentional pharmacological examinations, so it remains unknown how common BDMD might be in patients receiving standard levodopa medications. The present case suggests that a marked BDMD similar to the BDMD observed in intentional pharmacological examinations[12,13] can also occur in patients receiving standard doses of levodopa medications.

Beginning-of-dose motor deterioration has been accounted for on the basis of the inhibitory effects of levodopa, which suppress endogenous dopamine release and synthesis through predominant activation of presynaptic dopamine autoreceptors.[19,20,22] This hypothesis implies that BDMD may be induced by a dose of levodopa that is insufficient to activate postsynaptic dopamine receptors.[12,16] Management of BDMD may therefore be difficult in patients who are already receiving a relatively large dosage of levodopa, and when reducing the levodopa dosage in patients who are distressed by various side effects of the drug.

To the best of our knowledge, the present case demonstrates for the first time that BDMD can be inhibited by STN stimulation and further indicates the benefit of STN stimulation for managing the inhibitory effects of levodopa, if they are in fact responsible for the BDMD. In patients with PD, intraoperative microrecording has revealed that intravenous administration of apomorphine induces increased neuronal activities in both the STN[11] and the internal segment of the globus pallidus[7,13] during BDMD[11,13] and end-of-dose motor deterioration.[7] Such increased neuronal activities are also observed during wearing-off motor deterioration but are quantitatively more pronounced in that setting.[7,11,13] These findings suggest that motor deterioration in patients with PD is closely related to the activities of the basal ganglia, which result in an enhanced inhibitory input to the thalamus. Stimulation of the STN is suggested to suppress such abnormal neuronal activities underlying the PD symptoms[23] and to release the thalamus from excessive inhibition by the basal ganglia.[5,21] It is possible that BDMD and wearing-off motor deterioration are inhibited by STN stimulation through the same mechanism. The precise process whereby STN stimulation can improve on-off motor fluctuation remains to be elucidated. Both presynaptic and postsynaptic mechanisms have been postulated.[15,18] In a study on the interaction between deep brain stimulation and levodopa by Nutt et al.,[18] the improvement effect of acute STN stimulation (when patients were awake during the day) on wearing-off motor fluctuation was inferred to be due to a reduction of off-drug disability, and not alterations in the levodopa pharmacodynamics. This may suggest that the action of STN stimulation may be independent of striatal dopamine transmission; namely, a postsynaptic mechanism is primary. In contrast, Nimura et al.[15] demonstrated that chronic STN stimulation can induce stabilization of the striatal synaptic dopamine concentrations based on an [$^{18}$F]fluorodopa positron emission tomography study, and levodopa-related wearing-off motor fluctuation may thus be attenuated. The results of the positron emission tomography study indicate that the stabilization induced by STN stimulation involves a presynaptic mechanism. This is assumed to incorporate the following two main processes: 1) activated output from the motor and premotor cortex, which is induced by relaxant output from the STN via the pallidothalamocortical pathway, tending to attenuate dopamine release in the striatum, and 2) restoration of autoregulation in striatal presynaptic dopamine release through a feedback input from the STN to striatal somatodendritic autoreceptors. We inferred that a reduction of levodopa dosage may also contribute stability of striatal dopamine transmission. These combined mechanisms could facilitate further improvement in dopa-induced motor fluctuations with chronic STN stimulation.

## Conclusions

The present case confirms that STN stimulation can provide benefits in improving off-medication motor status through levodopa-like effects, through improving the on-medication motor status in patients who are intolerant to larger doses of levodopa, and through reducing the levodopa dose in patients who are distressed by various side effects of levodopa.[8] In addition, our observations suggest that STN stimulation has direct effects on some of the levodopa-induced motor symptoms, such as BDMD. The combination of chronic STN stimulation and reduction in dosage of levodopa may contribute further by improving levodopa-induced motor fluctuations through the stabilization of striatal dopamine transmission.





## References


1. Burchiel KJ, Anderson VC, Favre J, Hammerstad JP: Comparison of pallidal and subthalamic nucleus deep brain stimulation for advanced Parkinson's disease: results of a randomized, blinded pilot study. **Neurosurgery 45:**1375–1382, 1999
2. Contin M, Riva R, Martinelli P, Procaccianti G, Cortelli P, Avoni P, et al: Response to a standard oral levodopa test in Parkinsonian patients with and without motor fluctuations. **Clin Neuropharmacol 13:**19–28, 1990
3. Davis TL, Brughitta G, Baronti F, Mouradian MM: Acute effects of pulsatile levodopa administration on central dopamine pharmacodynamics. **Neurology 41:**630–633, 1991
4. Deep-Brain Stimulation for Parkinson's Disease Study Group: Deep-brain stimulation of the subthalamic nucleus or the pars interna of the globus pallidus in Parkinson's disease. **N Engl J Med 345:**956–963, 2001
5. Hashimoto T, Elder CM, Okun MS, Patrick SK, Vitek JL: Stimulation of the subthalamic nucleus changes the firing pattern of pallidal neuron. **J Neurosci 23:**1916–1923, 2003
6. Hughes AJ, Lees AJ, Stern GM: Apomorphine test to predict dopaminergic responsiveness in parkinsonian syndromes. **Lancet 336:**32–34, 1990
7. Hutchinson WD, Levy R, Dostrovsky JO, Lozano AM, Lang AE: Effects of apomorphine on globus pallidus neurons in parkinsonian patients. **Ann Neurol 42:**767–775, 1997
8. Katayama Y, Kasai M, Oshima H, Fukaya C, Yamamoto T, Ogawa K, et al: Subthalamic nucleus stimulation for Parkinson disease: benefits observed in levodopa-intolerant patients. **J Neurosurg 95:**213–221, 2001
9. Krack P, Batir A, Van Blercom N, Chabardes S, Fraix V, Ardouin C, et al: Five-year follow-up of bilateral stimulation of the subthalamic nucleus in advanced Parkinson's disease. **N Engl J Med 349:**1925–1934, 2003
10. Kumar R, Lozano AM, Kim YJ, Hutchison WD, Sime E, Halket E, et al: Double-blind evaluation of subthalamic nucleus deep brain stimulation in advanced Parkinson's disease. **Neurology 51:**850–855, 1998
11. Levy R, Dostrovsky JO, Lang AE, Sime E, Hutchison WD, Lozano AM: Effects of apomorphine on subthalamic nucleus and globus pallidus internus neurons in patients with Parkinson's disease. **J Neurophysiol 86:**249–260, 2001
12. Merello M, Lees AJ: Beginning-of-dose motor deterioration following the acute administration of levodopa and apomorphine in Parkinson's disease. **J Neurol Neurosurg Psychiatry 55:**1024–1026, 1992
13. Merello M, Lees AJ, Balej J, Cammarota A, Leiguarda R: GPi firing rate modification during beginning-of-dose motor deterioration following acute administration of apomorphine. **Mov Disord 14:**481–483, 1999
14. Moro E, Scerrati M, Romito LM, Roselli R, Tonali P, Albanese A: Chronic subthalamic nucleus stimulation reduces medication requirements in Parkinson's disease. **Neurology 53:**85–90, 1999
15. Nimura T, Yamaguchi K, Ando T, Shibuya S, Oikawa T, Nakagawa A, et al: Attenuation of fluctuating striatal synaptic dopamine levels in patients with Parkinson disease in response to subthalamic nucleus stimulation: a positron emission tomography study. **J Neurosurg 103:**968–973, 2005
16. Nutt JG, Gancher ST, Woodward WR: Does an inhibitory action of levodopa contribute to motor fluctuations? **Neurology 38:**1553–1557, 1988
17. Nutt JG, Holford NHG: The response to levodopa in Parkinson's disease: imposing pharmacological law and order. **Ann Neurol 39:**561–573, 1996
18. Nutt JG, Rufener SL, Carter JH, Anderson VC, Phawa R, Hammerstad JP, et al: Interactions between deep brain stimulation and levodopa in Parkinson's disease. **Neurology 57:**1835–1842, 2001
19. Paalzow GH, Paalzow LK: L-DOPA: how it may exacerbate parkinsonian symptoms. **Trends Pharmacol Sci 9:**15–19, 1986
20. Skirboll LR, Grace AA, Bunney BS: Dopamine auto- and postsynaptic receptors: electrophysiological evidence for differential sensitivity to dopamine agonists. **Science 206:**80–82, 1979
21. Welter ML, Houeto JL, Bonnet AM, Bejjani PB, Mesnage V, Dormont D, et al: Effects of high-frequency stimulation on subthalamic neuronal activity in parkinsonian patients. **Arch Neurol 61:**89–96, 2004
22. Westfall TC, Besson MJ, Giorgulieff MF, Glowinski J: The role of presynaptic receptors in the release and synthesis of $^{3}$H-dopamine by slices of rat striatum. **Naunyn Schmiedebergs Arch Pharmacol 292:**279–289, 1976
23. Wichmann T, DeLong MR: Functional and pathophysiological models of the basal ganglia. **Curr Opin Neurobiol 6:**751–758, 1996


Manuscript submitted June 2, 2005.
Accepted May 17, 2007.
This work was supported by grants from the Ministry of Education, Culture, Sports, Science, and Technology (Grant Nos. 12307029 and 15209047) and the Ministry of Education, Culture, Sports, Science, and Technology for the promotion of industry–university collaboration at Nihon University.

*Address correspondence to:* Hideki Oshima, M.D., Ph.D., Department of Neurological Surgery, Nihon University School of Medicine, Tokyo 173-8610, Japan. email: hoshima@med.nihon-u.ac.jp.